JOURNAL OF PETROLOGY | VOLUME 43 | NUMBER 6 | PAGES 1003–1028 | 2002

Cordieritite and Leucogranite Formation during Emplacement of Highly Peraluminous Magma: the El Pilón Granite Complex (Sierras Pampeanas, Argentina)

C. W. RAPELA[1]*, E. G. BALDO[2], R. J. PANKHURST[3] AND J. SAAVEDRA[4]

[1]CENTRO DE INVESTIGACIONES GEOLÓGICAS, UNIVERSIDAD NACIONAL DE LA PLATA, CALLE 1 NO. 644, 1900 LA PLATA, ARGENTINA

[2]UNIVERSIDAD NACIONAL DE CÓRDOBA, VELEZ SARSFIELD 299, CÓRDOBA, ARGENTINA

[3]BRITISH ANTARCTIC SURVEY, c/o NERC ISOTOPE GEOSCIENCES LABORATORY, KINGSLEY DUNHAM CENTRE, KEYWORTH, NOTTINGHAM NG12 5GG, UK

[4]INSTITUTO DE AGROBIOLOGÍA Y RECURSOS NATURALES, CSIC, CORDEL DE MERINAS 40–52, 38071 SALAMANCA, SPAIN

RECEIVED JUNE 8, 2001; REVISED TYPESCRIPT ACCEPTED JANUARY 5, 2002

*Cordieritites and highly peraluminous granites within the El Pilón granite complex, Sierras Pampeanas, Argentina, were emplaced during a medium-*P*, high-*T *metamorphic event during the initial decompression of a Cambrian orogen along the southwestern margin of Gondwana. Very fresh orbicular and massive cordieritite bodies with up to 90% cordieritite are genetically associated with a cordierite monzogranite pluton and a larger body of porphyritic granodiorite. The petrogenesis of this association has been studied using petrographical, mineralogical, thermobarometric, geochemical, geochronological and isotope methods. The granitic magmas were formed by anatexis of mid-crustal metamorphic rocks formed earlier in the Pampean orogeny. The cordieritites appear at the top of feeder conduits that connected the source region located at* ~ 6 *kbar with the pluton emplacement level at* $3{\cdot}7 \pm 0{\cdot}3$ *kbar. A fall in the liquidus temperature of the melt during emplacement was produced by a marked increase in fluid activity owing to rapid decompression and assimilation of surrounding hydrous metapelitic schists, followed by isobaric crystallization. High-Mg cordierite crystallized early on biotite–sillimanite restitic mineral assemblages of the assimilated schists or at the wall of the feeder conduits. Strong convection in the small magma chamber caused flow segregation of cumulate cordierite and restite, developing leucogranites and highly evolved pegmatoids that are in isotopic equilibrium. Rapid ascent of highly peraluminous magmas might explain why emplacement of these granites was simultaneous with the metamorphic peak registered in neighbouring high-grade migmatite and granulite terranes.*

KEY WORDS: *cordierite; anatexis; granite; geochemistry; Ordovician*

INTRODUCTION

Cordierite is a low-pressure mineral that appears above the granite solidus in many peraluminous felsic magmas and as a metamorphic (subsolidus) phase in pelitic rocks (Clarke, 1995). Both occurrences are typical of low-pressure (P), high-temperature (T) terranes that underwent extensive crustal melting in the late thermal stages of continental collision and terrane amalgamation. Examples are common in the Late Palaeozoic Variscan belt of Europe, the Cretaceous–Miocene Ryoke belt of Japan and the Cambrian Pampean belt of SW

Extended dataset can be found at http://www.petrology.oupjournals.org

*Corresponding author. E-mail: crapela@cig.museo.unlp.edu.ar

South America (Gardien *et al.*, 1997; Brown, 1998; Rapela *et al.*, 1998*a*).

The critical parameters controlling formation of cordierite in magmas are relatively low P, and high (Mg + Fe^{2+}), Mg/Fe^{2+}, alumina saturation index [ASI = $Al_2O_3/(CaO + Na_2O + K_2O)$ molar], aAl_2O_3, and fO_2 (Clarke, 1995). Cordierite is usually an accessory phase; in cordierite-bearing granites and rhyolites its abundance rarely exceeds 10% of the mode. Cordieritites, in which cordierite is a major mineral phase with >30 vol. %, are an extreme member of this rock family, and exceptionally approach an almost monomineralic composition with ~90% cordierite. In the case of a magmatic origin, such extreme compositions could be achieved only by some type of accumulation process after crystallization, and cannot be produced by metamorphism of a normal sedimentary protolith. If cordieritites are uncommon, orbicular cordieritites that share many of the field and fabric characteristics of orbicular granites are even rarer. Although they are curiosities in themselves, the petrogenesis of such rocks can shed light on many crucial aspects of granite magmatism, such as the composition of the source, the water content and the mechanism of emplacement of highly peraluminous magmas in low-P, high-T metamorphic belts. This is not a new idea; more than 70 years ago petrologists were surprised by the fact that in orbicular granites they faced many of the main problems of granite petrology 'almost literally, in a nutshell' (Sederholm, 1928).

The Cambrian granite complex of El Pilón in southern South America is composed of highly peraluminous igneous rocks and associated cordieritite bodies, emplaced during low-P, high-T metamorphism (Rapela *et al.*, 1998*a*). In particular, exceptionally fresh and well-exposed bodies of massive and orbicular cordieritite are closely associated with a small cordierite-bearing monzogranitic body. This paper focuses on the relationship between highly peraluminous granites and cordieritites in this setting. New field, mineralogical, chemical and isotopic data are presented to (1) constrain the P–T conditions of the source and emplacement of the granites, (2) determine the source of the highly peraluminous magmas and the roles of high-level partial melting and contamination, (3) identify the mechanism of magma ascent, and (4) evaluate the fractionation mechanism at the emplacement level that produced the observed accumulation of cordierites and chemical variations within the granite. Mineral abbreviations are those of Kretz (1983).

GEOLOGICAL SETTING

Palaeozoic basement rocks at 27–33°S (see insert, Fig. 1) may be subdivided into those related to Early to Middle Cambrian subduction and terrane collision (the Pampean mobile belt), and those associated with Ordovician subduction (the Famatinian mobile belt) and accretion of an exotic terrane (the Precordillera terrane) (see Pankhurst & Rapela, 1998). The Pampean mobile belt includes the Eastern Sierras Pampeanas and Eastern Cordillera geological provinces. It is mostly composed of metamorphic rocks (both high-grade and low- to medium-grade) and anatectic granites, partially remobilized and intruded by Ordovician–Carboniferous granitoids. The El Pilón granitic complex and associated cordieritites are located in the Sierras de Córdoba, in the southern part of the Pampean belt (Fig. 1), where the Cambrian events are well established (Rapela *et al.*, 1998*b*; Sims *et al.*, 1998, and references therein).

The Sierras de Córdoba are largely composed of metamorphic rocks, Cambrian to Devonian granitoid plutons emplaced at various levels, and subordinate basic and ultrabasic rocks (Fig. 1; Gordillo, 1984; Martino *et al.*, 1995; Baldo *et al.*, 1998; Rapela *et al.*, 1998*b*; Otamendi *et al.*, 1999). Cambrian metamorphic rocks of middle to high amphibolite facies are the main and most widespread component of the basement, in which large migmatitic masses are characteristic (see Rapela *et al.*, 1998*b*, fig. 1). Low-grade metapelites appear only along the western side of the sierras, whereas metabasic rocks crop out discontinuously in the central and southeastern areas. Garnet–cordierite migmatites dominate the lithology in most of the high-grade migmatitic massifs (Gordillo, 1984), a remarkable exception to which is that of El Pilón in the northwestern sector of the Sierras de Córdoba (Figs 1 and 2). Migmatites and granitoid rocks in this area define a large medium- to low-pressure, garnet-absent basement block, separated by major faults from other medium-pressure, garnet-bearing high-grade rocks to the south and east.

The history and timing of the local Early Palaeozoic events was established by Rapela *et al.* (1998*b*), whose conclusions are summarized here. Emplacement of a suite of metaluminous calc-alkaline granitoids at 530 ± 4 Ma (U–Pb on abraded zircons from three units) represents an active margin environment along the eastern edge of the Sierras Pampeanas. This magmatism was followed by crustal thickening that resulted in granulite facies conditions (P = 8·6 ± 0·8 kbar, T = 810 ± 50°C). A clockwise P–T–t path was inferred, producing regional migmatitic massifs during peak thermal conditions (M_2 metamorphic stage) at P = 5·7 ± 0·4 kbar, T = 820 ± 25°C; a monazite U–Pb SHRIMP age of 522 ± 8 Ma was thought to date the M_2 event. The P–T conditions of an earlier metamorphic stage (M_1) inferred from relict fabric in garnet cores could not be determined because of garnet homogenization during M_2. In the southern part of the Sierras de Córdoba, peak metamorphism occurred at essentially constant pressure of

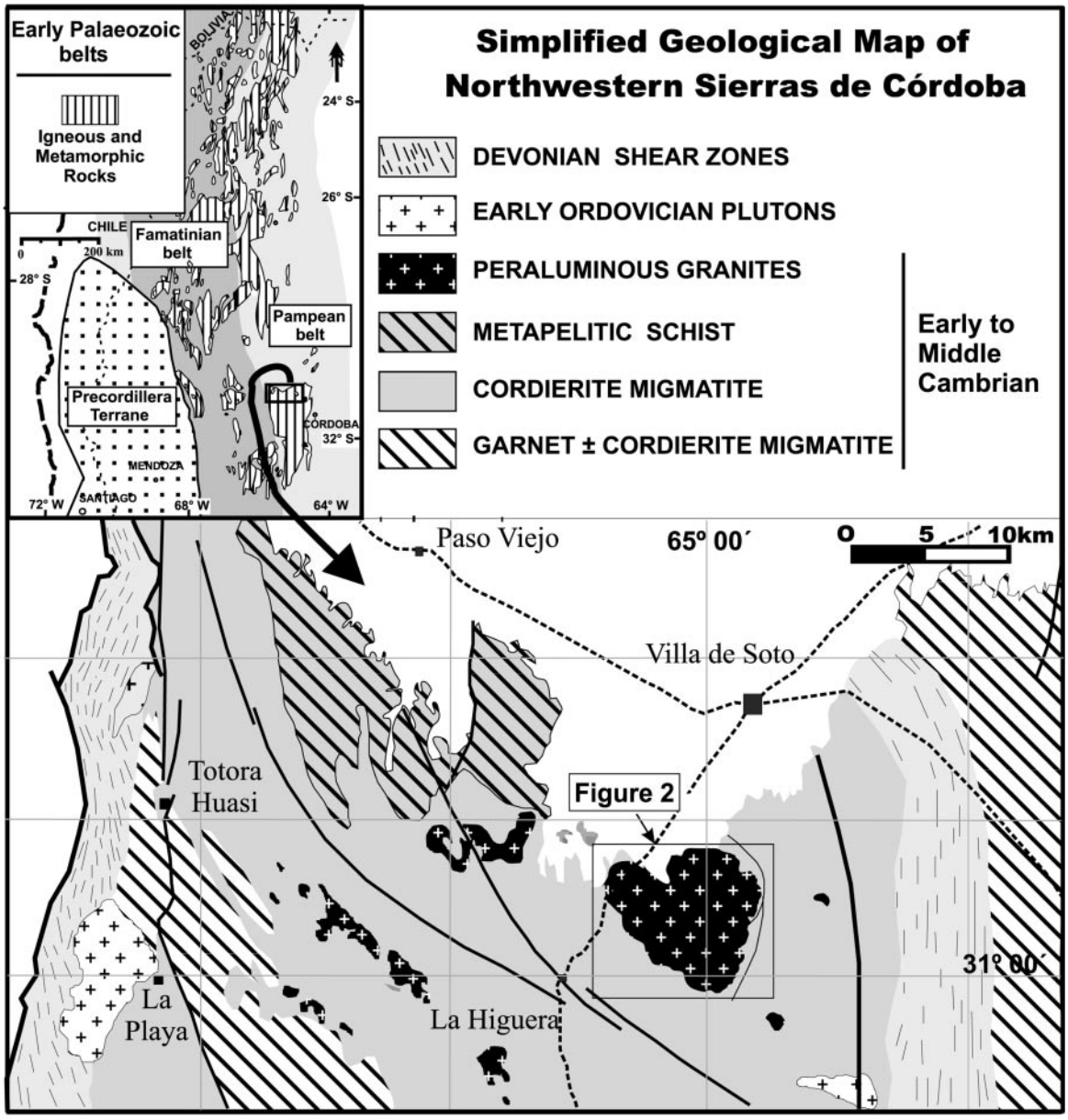

Fig. 1. Simplified geological map of the northwestern sector of Sierras de Córdoba [modified after Sims *et al.* (1998)]. Inset maps show the Early Palaeozoic belts of southern South America (Rapela *et al.*, 1998*b*) and the location of El Pilón granite complex.

7–8 kbar, with temperatures of ~800°C for the migmatites and ≥900°C for the granulites (Otamendi *et al.*, 1999). Strongly peraluminous cordierite–sillimanite granites, sometimes associated with cordieritites, as in the El Pilón complex, were emplaced coevally with the M_2 event at higher levels in the crust ($P = 3{\cdot}9 \pm 0{\cdot}6$ kbar, $T = 684 \pm 60$°C, Rapela *et al.*, 1998*b*). An undated M_3 event recorded in the migmatitic rocks ($P = 4 \pm 0{\cdot}5$ kbar, $T = 715 \pm 15$°C, Rapela *et al.*, 1998*b*), presumably corresponds to a stage during the exhumation of the high-grade rocks.

The igneous and metamorphic evolution of the Pampean belt has been interpreted in terms of collision between a continental block (the Pampean terrane) and Gondwana during early to mid-Cambrian times (Rapela *et al.*, 1998*a*, 1998*b*). The accreted terrane is envisaged as parautochthonous, related to the break-up scenario pertaining at the Precambrian–Cambrian boundary. Inherited zircon from the metapelitic high-grade migmatites as well as from the strongly peraluminous granites gives ages between 600 and 1400 Ma, suggesting provenance from a Mesoproterozoic to Neoproterozoic basement.

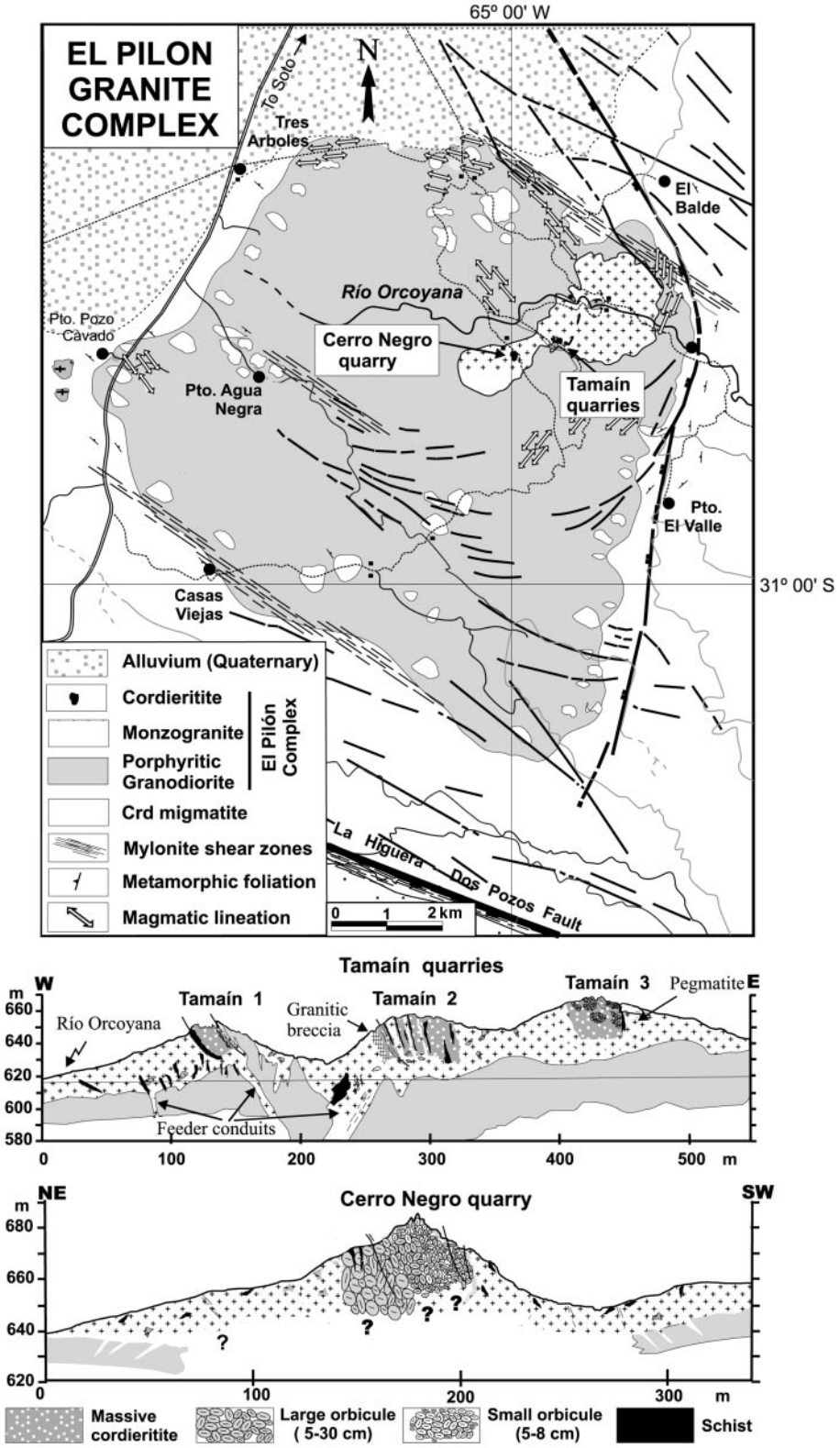

Fig. 2. Geological sketch map of El Pilón granite complex and cross-sections of the cordieritite bodies at the Tamaín and Cerro Negro quarries.

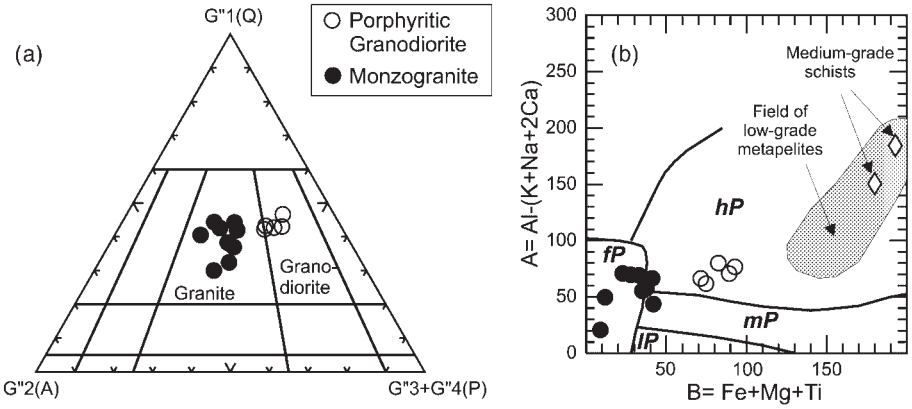

Fig. 3. Classification of the Cambrian granitic rocks of El Pilón complex. Chemical classifications relating to analysis of large samples (6–10 kg) are preferred, as in many cases the heterogeneous flow-fabric and coarse grain size prevent accurate modal measurements. (a) Multi-cationic homologue of the modal QAP triangle, after La Roche (1992). (b) Chemical classification of peraluminous granitoids (Villaseca *et al.*, 1998*a*): *hP*, highly peraluminous; *mP*, moderately peraluminous; *lP*, low peraluminous; *fP*, highly felsic peraluminous. Parameters are expressed as gram-atoms $\times$ 10^3 of each element in 100 g of rock.

The rock and mineral associations at El Pilón were first described by Gordillo (1974, 1979), and his work is a tribute to his pioneering research investigations in the cordierite-bearing rocks of the Sierras de Córdoba. Chemical analyses of the cordierites and granites of this area were performed and reported by Gordillo (1974, 1979), including a more focused study of sodian–beryllian cordierite (Schreyer *et al.*, 1979). New results at El Pilón reported in this study included mapping, major and trace element whole-rock geochemistry, mineral microprobe analysis, and Nd and Sr isotope determinations.

The 70 km^2 granitic complex of El Pilón is located in the central part of a middle- to low-pressure basement block defined by abundant cordierite–sillimanite migmatites, gneisses and schists with conspicuous cordierite and a lack of garnet in the high-grade rocks. The complex is subcircular, $\sim$10 km in diameter, and contains two main granitoid bodies (Figs 2 and 3): (1) a large porphyritic cordierite–sillimanite granodiorite pluton; (2) a small cordierite monzogranite body located in the NE sector of the complex. The latter encloses and is genetically associated with subcircular bodies of cordieritites. Subordinate tourmaline–cordierite pegmatoids are also spatially associated with the monzogranite.

THE METAMORPHIC ENVELOPE

Schists

Metapelitic muscovite schists located to the NW of the complex (Fig. 1) are the lowest-grade metamorphic rocks in the low-pressure basement block. The continuous outcrop is composed of medium- to low-grade schists dominated by pelitic layers having a mineral assemblage of Na-Crd poikilitic porphyroblasts (Na_2O 0·9–1·2%), Ms, Bt, Pl and Qtz. Staurolite is a relic phase that occurs as small crystals together with Bt and Ms within the Na-Crd porphyroblasts. Sandstone protoliths and impure quartzites alternate with the pelitic bands, and in these Qtz, Pl and Ms dominate the assemblage and Crd and St are absent.

Schist enclaves of all sizes are also very common in the porphyritic granodiorite and the cordierite monzogranite. The fabric and protolith composition of the enclaves are very similar to those of the *in situ* schists. However, primary muscovite has disappeared in most cases, and the dominant assemblage is Qtz + Bt + Pl + Kfs $\pm$ Sil $\pm$ Ms, suggesting an increase in metamorphic grade towards the El Pilón complex (Fig. 1). A summary of the metamorphic phase assemblages and mineral compositions in all metamorphic and granitic units is shown in Table 1. Th–U–Pb SHRIMP analysis of monazites from a biotite–muscovite gneiss located in the northwestern sector of the large schist outcrop gave an age of 526 $\pm$ 11 Ma, and U–Pb SHRIMP analysis of zircon rims from the same sample produced clusters at around 531 $\pm$ 10 Ma and 561 $\pm$ 10 Ma (Sims *et al.*, 1998). These data may be used to infer an age of 529 $\pm$ 7 Ma for the metamorphism in these rocks.

Migmatites

Cordierite migmatites are the dominant metamorphic lithology and are the host rocks of the peraluminous granites and the cordieritite. Stromatite and diatexite are the common types. The leucosome in the stromatites is composed of Qtz + Crd + Kfs $\pm$ Pl. The coarse-grained lepidoblastic melanosome contains Bt + Sil +

Table 1: Summary of metamorphic phase assemblages and mineral composition

	Schists		Migmatites			Cordieritite			Leucogranite/ porphyritic granodiorite	
	(1) (a) Qtz + Ms1 + Bt2 + Pl ± St (b) Crd2 + Bt2 + Ms2 ± And + Ilm		(1) Leucosome: Qtz + Kfs + Crd ± Pl			(1) Orbicular facies, restitic core: Bt + Sil + Crd1 + Pl + (Zrn + Ap)			(1) Restitic assemblages: (a) Bt1 + Sil + Crd1 + Grt (b) Bt1 + Sil + Crd1	
	(2) Qtz + Ms + Bt + Pl		(2) Mesosome: Qtz + Pl + Kfs + Bt + Sil + Ilm ± Crd			(2) Orbicular facies, granitic matrix: Qtz + Kfs + Pl			(2) Magmatic assemblages: Qtz + Pl + Kfs + Crd2 + Bt-2	
	(3) Qtz + Bt + Pl + Kfs ± Sil ± Ms		(3) Melanosome: Bt + Sil + (Ap + Tur)			(3) Massive facies: (a) poikilitic Grt with Bt1 + Qtz + Ap inclusions and (b) Crd2 + Bt2 + Pl corona				
	(1)	(2)	(1)	(2)	(3)	(1)	(2)	(3)	(1)	(2)
mg-no. Crd1			61–63		64	69–72		67–68	59–61	
mg-no. Crd2	64–65					65–67		65–66		50–62
mg-no. Bt1	48–49	43–44						66–67	42–44	44–50
mg-no. Bt2	57–59		49–51	44	44–46	50–52		49–50		
mg-no. St	18–20									
mg-no. Grt core								22–23	11–12	
mg-no. Grt rim								13–14	9–11	
An Pl core	22–26	23	20		21		16–20	25	20–24	19–19
An Pl rim		27	18			18		27		

Tur + Ap, with fibrolite along the leucosome–melanosome interface. A hexagonal granoblastic aggregate of Pl + Kfs + Bt + Sil + Ilm ± Crd is typical of the mesosome.

Heterogeneous diatexites with nebulitic and agmatitic structures have nodular cordierite (5–10 cm), and in some cases grade into porphyritic Sil + Crd granite. The granoblastic texture of the diatexites, which are composed of Qtz + Pl + Bt + Crd + Sil ± Kfs (secondary Ms + Chl), is sometimes modified by ductile shear deformation that also affected the peraluminous granites. Cordierite + tourmaline-bearing pegmatoids and tourmaline pegmatites are common near the El Pilón complex.

EL PILÓN GRANITE COMPLEX

The porphyritic granodiorite

The largest granitic intrusion at El Pilón is a 63 km^2 porphyritic granodiorite pluton characterized by an abundance of enclaves of the country rock migmatites and schists, which range from a few centimetres to >50 m (Fig. 2). On the regional scale the contact of the granodiorite with the country rock migmatites is sharp, but at outcrop scale it is transitional over a few metres, with an increasing proportion of country rock enclaves in the granite. Small cordierite-bearing pegmatoids occasionally cut the porphyritic granodiorite. K-feldspar phenocryst, biotite-rich schlieren and metamorphic enclaves orientated subparallel to the contact suggest local flow of the granodiorite magma. There is no thermal contrast between the granodiorite and the high-grade country rocks, and the abundance of metamorphic enclaves suggests that the present level of erosion was near the roof of the granite pluton (Gordillo, 1974). K-feldspar phenocrysts (Or_{90}, length 1–7 cm, average 2 cm) are poikilitic, carrying euhedral plagioclase, biotite, and quartz, or occasionally only sillimanite. Plagioclase, biotite, prismatic sillimanite and subhedral altered cordierite are the remaining dominant mineralogy, with apatite and zircon as accessory minerals. Cordierite is very abundant and appears as either anhedral crystals included in Kfs phenocrysts associated with Sil, Bt and Qtz, or as isolated, inclusion-free, partially pinnitized individuals, indicating that the porphyritic granodiorite is mineralogically a strongly peraluminous granite (Miller, 1985). Occasionally cordierite also occurs as nodules up to 10 cm in diameter. Microscopic clusters of Bt + Sil + Grt + Crd ± Qtz are characteristic; they have a lepidoblastic fabric and are hence interpreted as restitic rather than glomerocrystic. Migmatitic enclaves in the porphyritic granodiorite show garnet-absent restitic melanosomes (Bt + Sil + Crd).

A precise emplacement age of 523 ± 2 Ma for the porphyritic granodiorite facies was obtained by conventional U–Pb analyses of zircon, whereas discordant fractions suggest Proterozoic inheritance (Rapela *et al.*, 1998*a*).

The cordierite monzogranite

A NE-trending monzogranitic body clearly intrudes the porphyritic granodiorite in the NE sector of the complex (Fig. 2). This small body of ~4 km^2 is composed of two small lenses, each displaying a subcircular shape in plan view, connected by a narrow zone of 200 m width. Despite the relatively reduced scale of the vertical exposures at El Pilón, the three-dimensional shape of the bottom of the monzogranite body and the associated cordieritite bodies can be reasonable inferred as a result of two fortuitous circumstances. The present erosion level is near the floor of the body, so that river sections, especially along the Río Orcoyana, allow direct observations. Moreover, spatial relationships at this level are exceptionally well exposed, as all the cordieritite bodies and several sites in the monzogranite have been intensively quarried for ornamental purposes. Erosional windows in small creeks and dry gullies show that the porphyritic granodiorite is always present at the floor of the monzogranite. From these observations, especially in the cross-section at Tamaín 2 quarry (Fig. 2), it is clear that the floor of the monzogranite is nearly flat, and extended laterally over the granodiorite during emplacement. The top of the body was located above the present level of erosion so that its thickness cannot be directly measured. However, the abundance of large schist enclaves, similar to those cropping out 14 km NW of the complex, in both the monzogranite and the cordieritites, suggests that the roof of the body was close and the monzogranite was emplaced as relatively thin, subhorizontal intrusion between the porphyritic granodiorite and the schists. Fabric evidence suggests that the underlying granodiorite was still ductile at the time of intrusion, although irregular-shaped 'xenoliths' of the granodiorite in the monzogranite often found near the contact clearly indicate that the latter was a late intrusive event within the granitic complex.

The grain size of the monzogranite is fine to medium, rarely exceeding 4 mm. Anhedral K-feldspar (Or_{90}) with abundant sillimanite and pinnitized cordierite inclusions, small amounts of biotite, and cordierite partially retrogressed to biotite + sillimanite are the main minerals. Common accessories are zircon and apatite. Small (5–7 cm) restitic ovoid clusters of Bt + Sil + Grt + Crd ± Qtz are common, as well as pegmatoid patches and veins (Table 1). The restitic almandine-rich garnets contain orientated inclusions of Bt, Qtz and Ilm, and are often rimmed by Crd and Bt, indicating retrograde

adjustment. Whereas modal biotite varies from 8 to 15% in the main facies of the body, there is sometimes a local decrease to <5%, noticeable for example in the colour index of the leucogranites and pegmatoids spatially associated with the cordieritites of the Cerro Negro quarry (Fig. 2). Close to the southern contact of the body, the country rock migmatites and schists desegregate into the monzogranite, leaving subcircular melanosome clusters of Bt + Sil.

The cordieritites

At the tops of small hills there are four outcrops, each up to 40 m × 80 m in length, of a cordierite-rich rock enclosed within the monzogranite body (Fig. 2). Three of these (Tamaín quarries 1, 2, and 3) occur in the southern part of the eastern subcircular lens of the body, and the remaining outcrop is in the western monzogranite lens (Cerro Negro quarry). This exceptional rock, consisting of 70–95% cordierite, has been called *cordieritite* (Gordillo, 1979; Schreyer *et al.*, 1979). Because of its beautiful pale blue colour, the cordieritite outcrops have been intensively quarried as ornamental stone and exported to Europe since the early 1950s (Gordillo, 1974).

Two main facies—orbicular and massive—are recognized, called respectively 'dark' and 'light' varieties by Schreyer *et al.* (1979). The Cerro Negro quarry is made up entirely of a remarkable orbicular cordieritite consisting of 5–30 cm egg-shaped orbicules, often rimmed by a thin aggregate of biotite and fibrolite. Orbicules are composed of a light-coloured shell and a dark core [Fig. 4a; terminology for the orbicule structure follows that of Leveson (1966)]. The shell is essentially monomineralic, consisting of a polycrystalline aggregate of polygonal, fresh cordierite, with chlorite and fibrolite surrounding individual crystals, and with minor quartz, plagioclase, dumortierite, apatite and zircon. The largest orbicules (>20 cm) have high shell/core ratios and the shells display a grain-size zonation in which the individual cordierite crystals decrease from 1–7 mm around the core to a fine-grained outer layer (Fig. 4c). Outer parts of the core are often irregular and partially digested into the innermost layer of the shell. Small orbicules (<5–8 cm) usually show unzoned, uniform cordierite shells, and lower shell/core ratios.

The dark core of the orbicules is mainly composed of oriented biotite, sillimanite, and cordierite, with subordinate amounts of feldspar, quartz, ilmenite and secondary muscovite and chlorite. Despite the appropriate aluminous composition, garnet has never been found in the orbicule cores. The fabric and mineralogy of the orbicular cores in the Cerro Negro outcrop are indistinguishable from the melanosome of the regional cordierite migmatites. Restitic cores are usually elongated, but rounded, semi-rectangular or irregular shapes are also observed, in which cases the external cordierite mantles reflect the shape of the core. The space between orbicules is occupied by small patches of a leucogranitic matrix composed of quartz, perthitic K-feldspar and plagioclase (Fig. 4a and b).

In the Cerro Negro quarry, large orbicules in a 'matrix' of smaller orbicules (Fig. 4c) are observed in the lower part of the 30 m cross-section, in contact with the monzogranite. There is an upward decrease in size equivalent to 'graded bedding' (Fig. 5). The lower zone is dominated by large orbicules (long axis 8–15 cm) although smaller and larger ones are also present. In the middle zone there is a general decrease in the size, and the mode is between 7 and 8 cm. The top of the section is composed solely of small oriented orbicules (all <11 cm, >50% in the range 4–6 cm). At the very bottom of the section, the leucogranitic matrix increases in proportion towards the contact with the granite, resulting in orbicules 'swimming' in the enclosed leucogranite (Fig. 4b). Isolated orbicules are found in the local leucogranite up to 4 m away from the contact, but they have never been observed in other parts of the monzogranitic body.

In the Tamaín quarries 2 and 3, small orbicules are single crystals with a small, limpid cordierite core, surrounded by a cordierite shell with concentrically arranged deformed inclusions, suggesting growth of the latter in a partially molten host (Gordillo, 1979). Microprobe analysis of the inclusions indicates that they consist of apatite. The fabric of the orbicules suggests that they grew epitaxially following nucleation around either partially melted biotite-rich restite or large idiomorphic crystals of cordierite. Accumulation of orbicules that seem to have been deformed and accommodated to each other in a ductile way, presumably in a fluid matrix, is typical of the orbicular facies (Fig. 4). The outer rims of large orbicules are sometimes digested and deformed by 'impacts' of small orbicules during the process of accumulation (Fig. 4c).

The Tamaín 1 and Tamaín 2 quarries are dominated by a massive cordieritite facies, which approaches a composition of almost monomineralic cordierite (85–90%) with Bt, Pl, Kfs and Qtz making up the remaining 10–15%. Coarse- and fine-grained varieties, with sharp contacts between them, are typical of the massive facies. In some sectors the massive cordieritite shows a gradual transition to darker varieties with up to 40% of modal biotite. The cordierite is fresh, and in the coarse variety forms a polycrystalline aggregate of 1–3 cm phenocrysts, with cyclic twins set in a groundmass of small crystals (0·5–2·5 mm), and with fibrolite and biotite at the crystal edges. Rare porphyroblastic garnet was observed only in the fine-grained variety of the Tamaín 2 quarry (see below), whereas staurolite appears in the more biotitic variants. Apatite is very abundant in the fine-grained

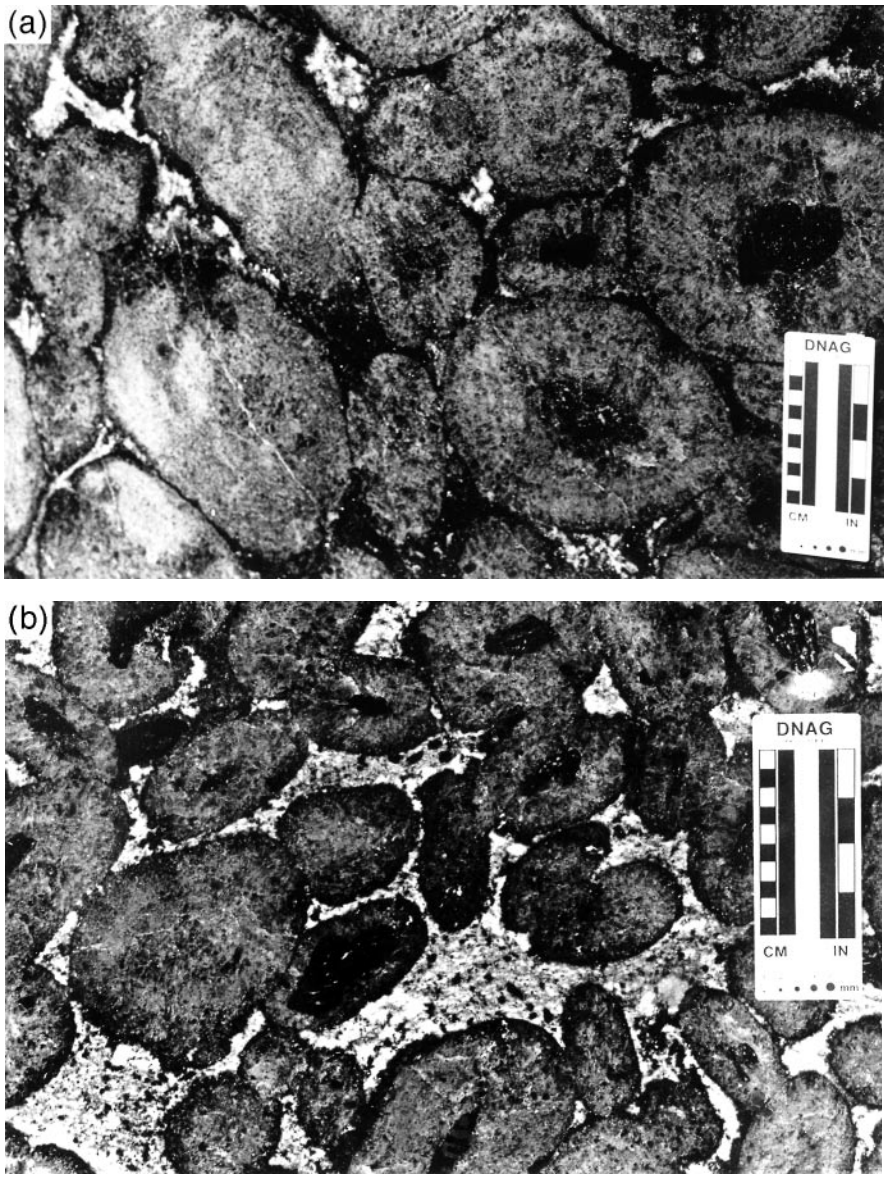

Fig. 4.

massive cordieritite; tourmaline, zircon and less frequently piedmontite, dumortierite and pyrite are also present. In the Tamaín 3 quarry, the fine-grained massive cordieritite is in sharp contact with the orbicular facies, consisting here of small orbicules with cordierite cores. The massive cordieritite of Tamaín 2 displays sharp magmatic-style contacts against both the granite and screen-like exposures of schist (Bt + Qtz + Pl + Kfs). This facies also contains a large (1 m × 1·5 m) xenolith of the porphyritic granodiorite, indicating that the massive cordieritite was ductile enough to be mobilized together with the monzogranite melt. A breccia facies seen in the Tamaín 2 quarry has angular xenoliths of the granodiorite, schists and subordinate cordieritite set in the monzogranite matrix, suggesting that local fluid-rich turbulent flow of the monzogranite melt affected both the cordieritite and the host granitic and metamorphic rocks. Although the exposures in the Tamaín quarries are small, the observed relations suggest that the massive cordieritite was not formed by an *in situ* accumulation as is deduced for the orbicular variety of the Cerro Negro quarry.

Cross-sections of the cordieritite bodies show that both types have restricted vertical continuity and are spatially associated with funnel-shaped vertical dykes of the monzogranite that terminate at the floor of the body (Fig. 2). An obvious interpretation of these spatial relationships, further discussed below, is that these dykes were feeder conduits of the monzogranite lenses.

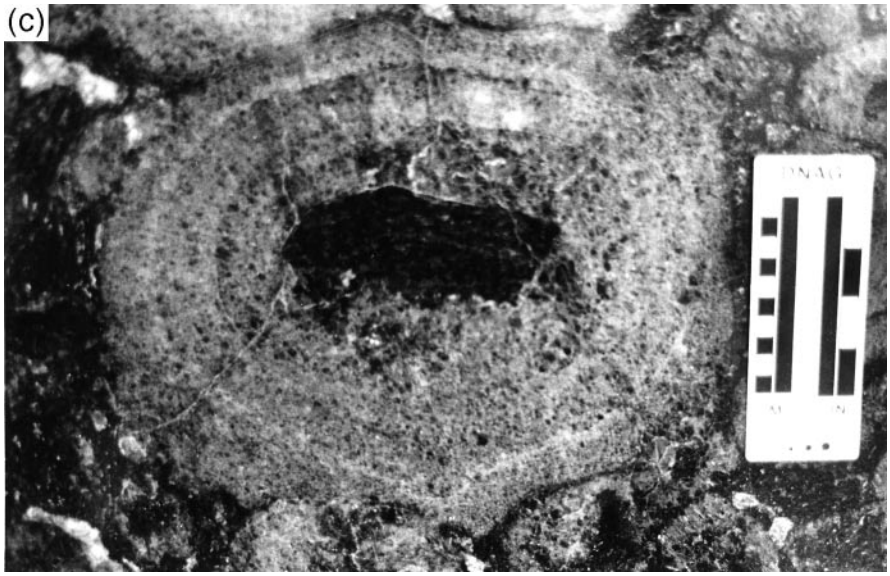

Fig. 4. Photographs of slabbed surfaces of orbicular cordieritite from Cerro Negro, El Pilón granite complex. (a) Ellipsoidal orbicules composed of a cordierite shell and a dark core of Bt + Sil + opaque minerals. The slab surfaces do not always intersect the orbicule cores, which are, however, present in all cases. A leucogranitic matrix of K-feldspar, quartz and plagioclase fills the space between orbicules, which (b) increases towards the contact with the host monzogranite. (c) A 30 cm orbicule set in a matrix of smaller orbicules at the base of the Cerro Negro section. The following features should be noted: (1) the indentation of the shell structure by neighbouring orbicules; (2) the decreasing size of the cordierite crystals towards the edge of the shell of the large orbicule; (3) the partially digested outer part of the core.

P–T CONDITIONS AT THE EMPLACEMENT LEVEL AND IN THE SOURCE REGION OF THE CORDIERITITE PARENTAL MAGMAS

The porphyritic granodiorite of the El Pilón granitic complex is emplaced in stromatitic and diatexitic Crd migmatites, whereas the monzogranite, which has abundant schist enclaves, was emplaced between the medium-grade schists and the migmatites. The emplacement depth of the monzogranite and associated cordieritites, as well as the *P–T* conditions in the source region of the granitic magmas, have been estimated from thermobarometric calculations in the cordieritite and in Bt–Sil–Grt restitic assemblages in the monzogranite (samples PIL-375 and PIL-202, Table 1).

Although garnet is a common mineral in the restitic assemblages, it was never found in the restitic cores of the Cerro Negro orbicular cordieritites, indicating that the latter are partial melting residues formed above the garnet stability field, probably remaining from assimilation reactions at the level of emplacement. The only exception is a resorbed garnet crystal discovered in the cordieritite of the Tamaín 2 quarry (Fig. 2), where the association Grt–Crd–Sil–Bt–Qtz–(St–Ap–Tur–Ilm–Zrn–dumortierite) was found in an angular enclave of fine-grained cordierite set in a groundmass of orbicular cordierite with euhedral cores. A large enclave of the granodiorite also occurs here in the massive cordieritite. The studied sample (PIL-375) shows a granoblastic texture of euhedral 0·3–0·5 mm crystals of limpid cordierite (Crd1) with inclusions of fibrolite, and surrounded by smaller crystals of cordierite, plagioclase and quartz. An isolated 9 mm garnet crystal is partially resorbed at the edge by the growth of an anhedral and poikilitic cordierite (Crd2) (Fig. 6a), with inclusions of biotite, quartz and fluorapatite. Apatite is very abundant and occurs as inclusions in all major minerals, suggesting that Grt and Crd1 formed during the same process in contact with melt and apatite crystals.

Chemical profiles of the garnet show compositional plateaux in the central part of the crystal and marked zonation at the edge, with an increase in Alm, Spl and the Fe/(Fe + Mg) ratio, and a decrease in Prp towards the rim (Fig. 6b). The unzoned core is a remnant of the original garnet, probably preserved because of the large size of the crystal (~10 mm). This type of rim zonation is usually ascribed to inward diffusion of Fe, Mg and Mn in retrograde reactions during decompression (Spear *et al.*, 1999). The main reaction consuming garnet to form the poikilitic Crd2 at the edge of crystal was

$$2\ \mathrm{Grt} + 4\ \mathrm{Sil} + 5\ \mathrm{Qtz} = 3\ \mathrm{Crd}.$$

Although Ca distribution is less well defined, Ca decreases in the garnet at the garnet–plagioclase contacts, whereas it increases towards the edge in the plagioclase crystals (up 2% An), suggesting that partition of Ca between the two minerals was produced by the reaction

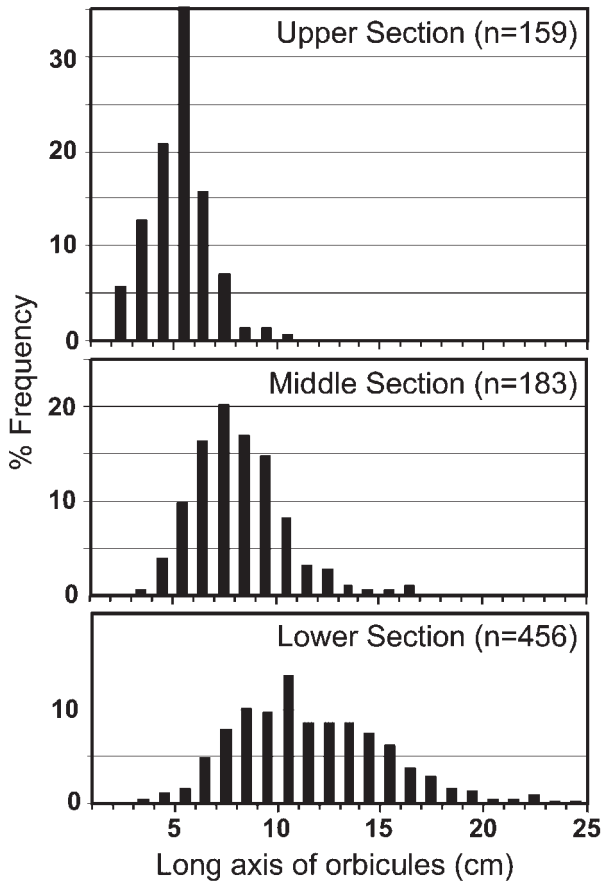

Fig. 5. Size distribution of orbicules through the vertical section in the Cerro Negro quarry.

$$\text{Grs} + \text{Sil} + \text{Qtz} = 3\ \text{An}.$$

Two paragenetic mineral associations were selected according to the above textural relationships and considerations, to infer the *P–T* conditions prevailing in the two stages of the evolution of the rock. The first is composed of the Grt core + Pl core + Crd1 (Paragenesis 1), and represents the equilibrium attained during the maximum *P–T* conditions. The second is composed of the Grt rim + Pl rim (in contact with Grt) + Crd2 + Bt (in contact with Grt) (Paragenesis 2), and represents local equilibrium during the formation of cordierite at lower *P–T* conditions. *P–T* conditions were calculated with version TWQ/102 of TEEWQ (Berman, 1991). Solid solution models are those from McMullin *et al.* (1991) for Bt, Berman (1991) for Grt, and Fuhrman & Lindsley (1988) for Pl, and an ideal model for Crd was assumed. The calculations for Paragenesis 1 were restricted to H_2O-conserving equilibria, thus constraining *P–T* conditions independently of water activity. However, it is clear that anatexis at 6–8 kbar in the Sierras de Córdoba took place in water-undersaturated conditions, either with a small amount of free water or with dehydration melting of biotite (Otamendi & Patiño Douce, 2001). For estimating the *P–T* conditions of Paragenesis 2 at the emplacement level, a high water activity ($a\text{H}_2\text{O} \sim 1$) was assumed. This is consistent with the estimates in the restite of the monzogranite (sample PIL-202), where equilibrium in the reaction set is optimum only for the interval $a\text{H}_2\text{O} = 0{\cdot}9$–$1{\cdot}0$. The mineral chemistry data on which these calculations are based are given in Appendix 1, available from the *Journal of Petrology* Web site (http://www.petrology.oupjournals.org). The two independent sets of calculated reactions intercept in tightly restricted *P–T* fields (Fig. 6c and d), suggesting that chemical equilibrium was attained in both textural assemblages. Estimated mean *P–T* values can be therefore considered representative of the physical conditions prevailing during formation of the respective paragenetic mineral association (Fig. 6c and d).

The values of 780°C and 5·9 kbar obtained for the restitic Paragenesis 1 in the massive cordieritite indicate a first generation of Crd + Grt at ~20 km depth. These *P–T* estimates may be compared with those obtained by similar methods in other Crd + Grt migmatitic massifs formed during the M_2 episode in the Sierras de Córdoba (Fig. 7). Paragenesis 1 conditions are below those obtained in the southern sector (Otamendi *et al.*, 1999) and within the range, but close to the lower limit of those in the central–east sector (Rapela *et al.*, 1998*b*). Thus the *P–T* values obtained for the paragenesis of the massive cordieritite suggest that the garnet-bearing restitic associations observed in the granitoids and the cordieritites of El Pilón (Table 1) are samples from a deeper mid-crustal source region (Fig. 7).

P–T conditions inferred for Paragenesis 2 (650 ± 16°C, 3·7 ± 0·3 kbar) plot on the haplogranite water-saturated solidus, suggesting that crystallization ends during near water-saturation conditions (Fig. 7). The calculated pressure range most probably represents re-equilibration conditions at the emplacement level of the cordieritite and the peraluminous granites (~10–15 km depth, Fig. 7). This range is consistent with that estimated in the country rock migmatites (3·9 ± 0·6 kbar, Rapela *et al.*, 1998*a*). Furthermore, the lack of primary magmatic muscovite in the monzogranite indicates that crystallization took place below the invariant point in the KFMASH system where the reaction products in the reaction Ms + Qtz = Sil + Kfs + coexist with granitic melts (see Fig. 7).

The pressure of 3·3 ± 0·6 kbar estimated for a garnet-bearing restite in the monzogranite is slightly lower than that obtained for Paragenesis 2 (sample PIL-202, Fig. 6e). This association exhibits a lepidoblastic texture, with Bt and Sil orientated as a relict metamorphic foliation. The xenoblastic garnets are surrounded by Bt + Sil

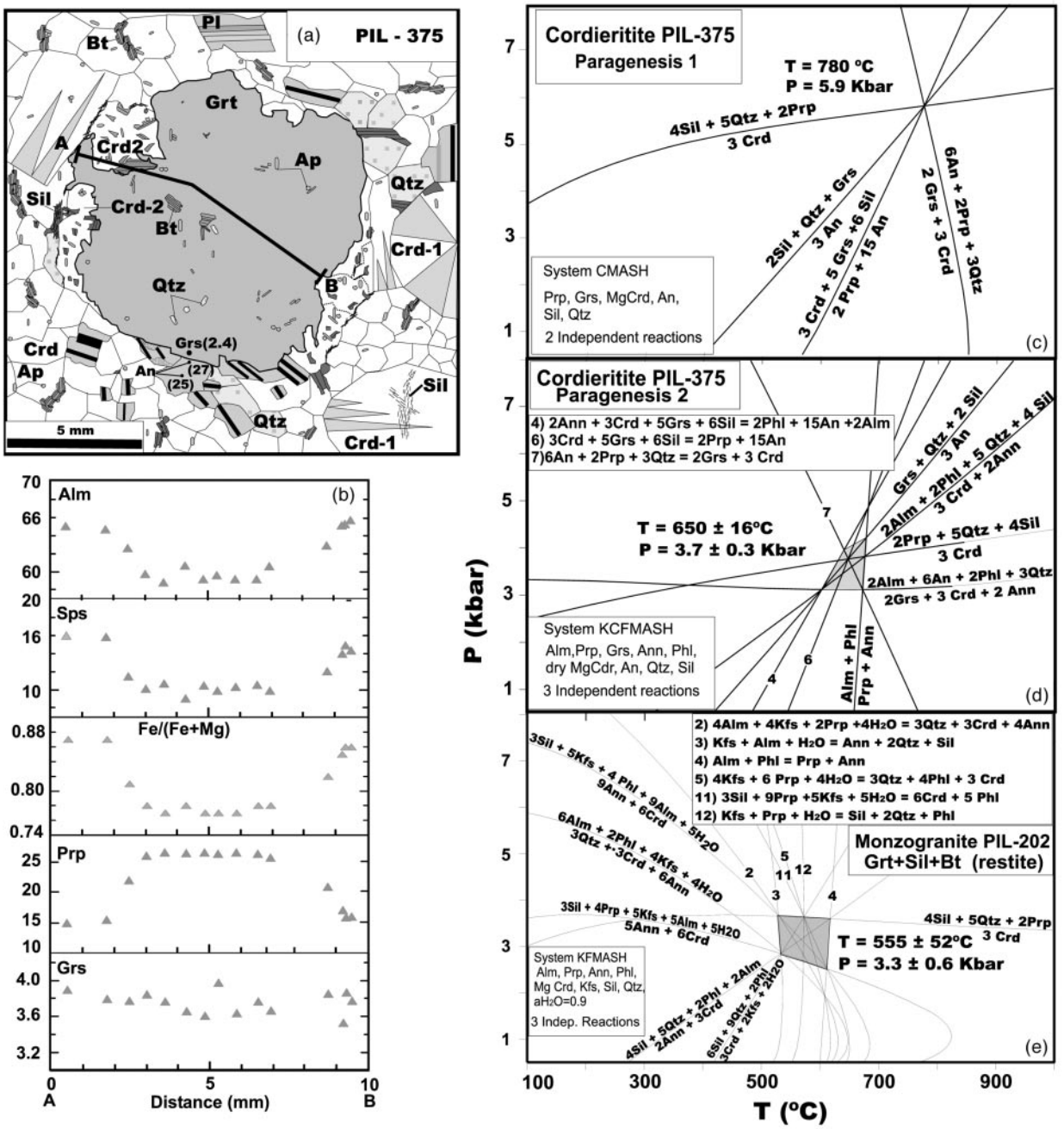

Fig. 6. (a) Restitic Grt–Crd in cordieritite PIL-375. Large Grt crystal overgrown by xenoblastic Crd2, in a matrix composed of Qtz, limpid Crd1, Pl, Sil and Bt. (b) Electron microprobe traverse across Grt as shown in (a). See text for discussion. (c) *P–T* conditions for Grt core + Pl core + Cdr1 (Paragenesis 1) of cordieritite PIL-375. (d) *P–T* conditions for Grt rim + Crd2 + Bt2 (Paragenesis 2) cordieritite PIl-375. [See (a) for textural relationships.] (e) *P–T* conditions for the restitic association Grt (xenoblastic) + Crd + Bt + Sil in sample PIL-202 of the monzogranite.

and, eventually, Crd, suggesting that the main reactions consuming garnet were

$$\text{Kfs} + \text{Grt} + \text{Melt} = \text{Sil} + \text{Bt} + \text{Qtz}$$

and

$$\text{Grt} + \text{Qtz} + \text{Sill} + \text{Melt} = \text{Crd} + \text{Bt}.$$

The estimated temperature for the restitic association plots below the temperature of the wet haplogranitic solidus at the given pressure (Fig. 7), and probably

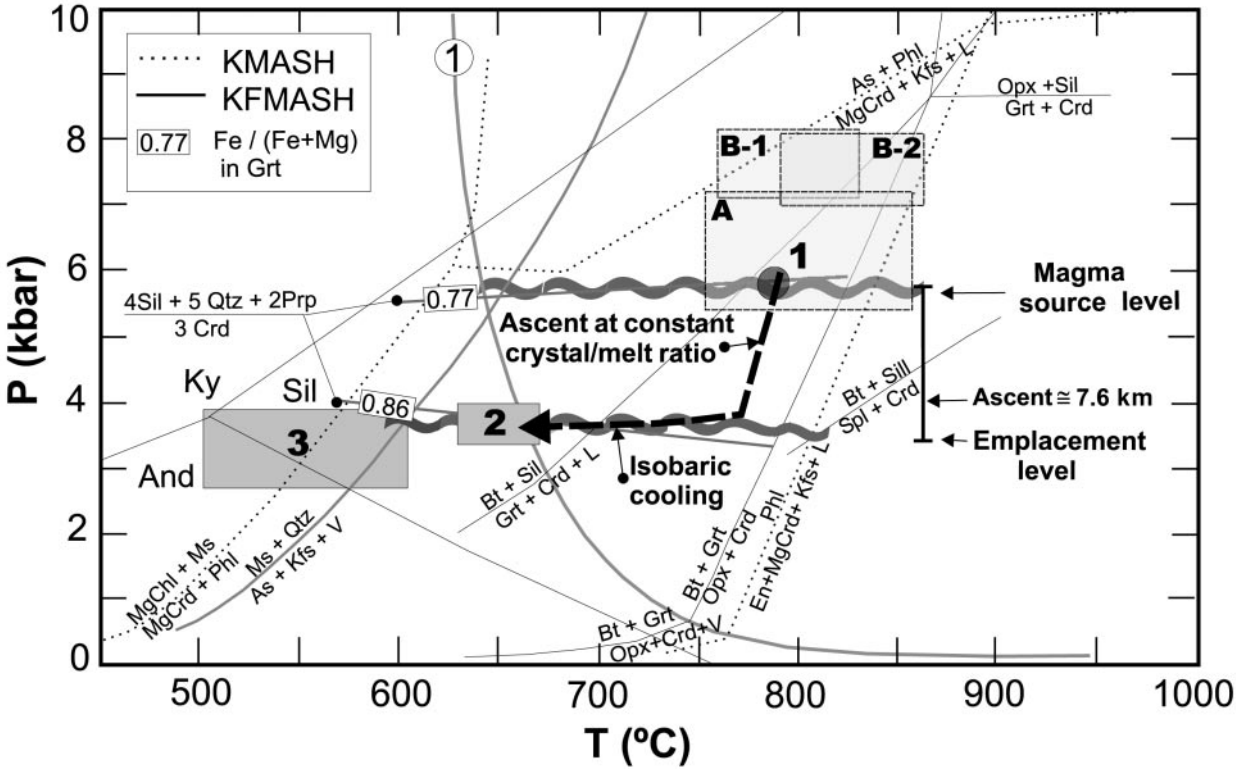

Fig. 7. Synthesis of *P–T* conditions for the Sierras de Córdoba. Dark shaded circle and boxes: representative samples of the cordieritite and the monzogranite from El Pilón complex (this work). 1, *P–T* estimate for the source region of the highly peraluminous magmas; 2, *P–T* estimate for the emplacement level of the magmas and the final temperature of crystallization of the cordieritites; 3, subsolidus adjustment of the restitic assemblage at the emplacement level. The bold dashed line with arrow shows the *P–T* ascent path of a granitic magma with a constant crystal/melt ratio and a starting melt fraction of 90%, followed by isobaric cooling at the emplacement level. Shaded boxes give estimates of the *P–T* conditions reached in different migmatitic massifs. A, Grt + Crd migmatites of Río Suquía (Rapela *et al.*, 1998*a*); B-1 and B-2, Grt and Grt + Crd migmatites of the Sierra de Comechingones (Otamendi *et al.*, 1999). The main melting reactions in the systems KFMASH and KMASH are after Spear *et al.* (1999). Aluminosilicate phase diagram as given by Berman (1991). Circled '1', haplogranitic water-saturated solidus.

represents a subsolidus, minimum temperature for the equilibrium exchange between Grt, Bt and Crd.

GEOCHEMISTRY

The granites of the El Pilón complex belong to the series with the highest peraluminosity in the classification of peraluminous granites (Fig. 3b). The porphyritic granodiorite is of the highly peraluminous type, which defines a trend from the most mafic varieties towards the field of metapelites. The monzogranite pluton mostly plots in the field of highly felsic peraluminous granites, but the main facies with >10% modal biotite is transitional to the highly and moderately peraluminous fields.

Selected major and trace element variations in the peraluminous granites, cordieritites and metamorphic rocks of El Pilón are illustrated in Figs 8–11; representative whole-rock analyses are given in Appendix 2 (available from the *Journal of Petrology* Web site). Different symbols are used to differentiate the orbicular and massive facies of the cordieritites, as well as single whole-rock analysis of an orbicule core and matrix from Cerro Negro. Two representative samples of the medium-grade metapelitic muscovite schists from NW of El Pilón complex (Fig. 2) illustrate the probable original composition of the partially digested schist enclaves observed in the monzogranite and the cordieritites. The composition of these schists falls in the field of the regional low-grade metapelitic rocks of the Sierras the Córdoba, also shown in Fig. 8. Low-grade metapelitic rocks are located 50 km to the SW of El Pilón [for chemical and Sr–Nd isotopic analyses of these rocks, see Rapela *et al.* (1998*a*)].

Elements such as MgO, FeO and Na_2O define linear plots between the granites of El Pilón, with the cordierite monzogranite of El Pilón as the most acidic unit, and the orbicular cordierites, with the nuclei as the least evolved member (Fig. 8). Although the scatter is larger for other elements, a main feature of the Harker diagrams

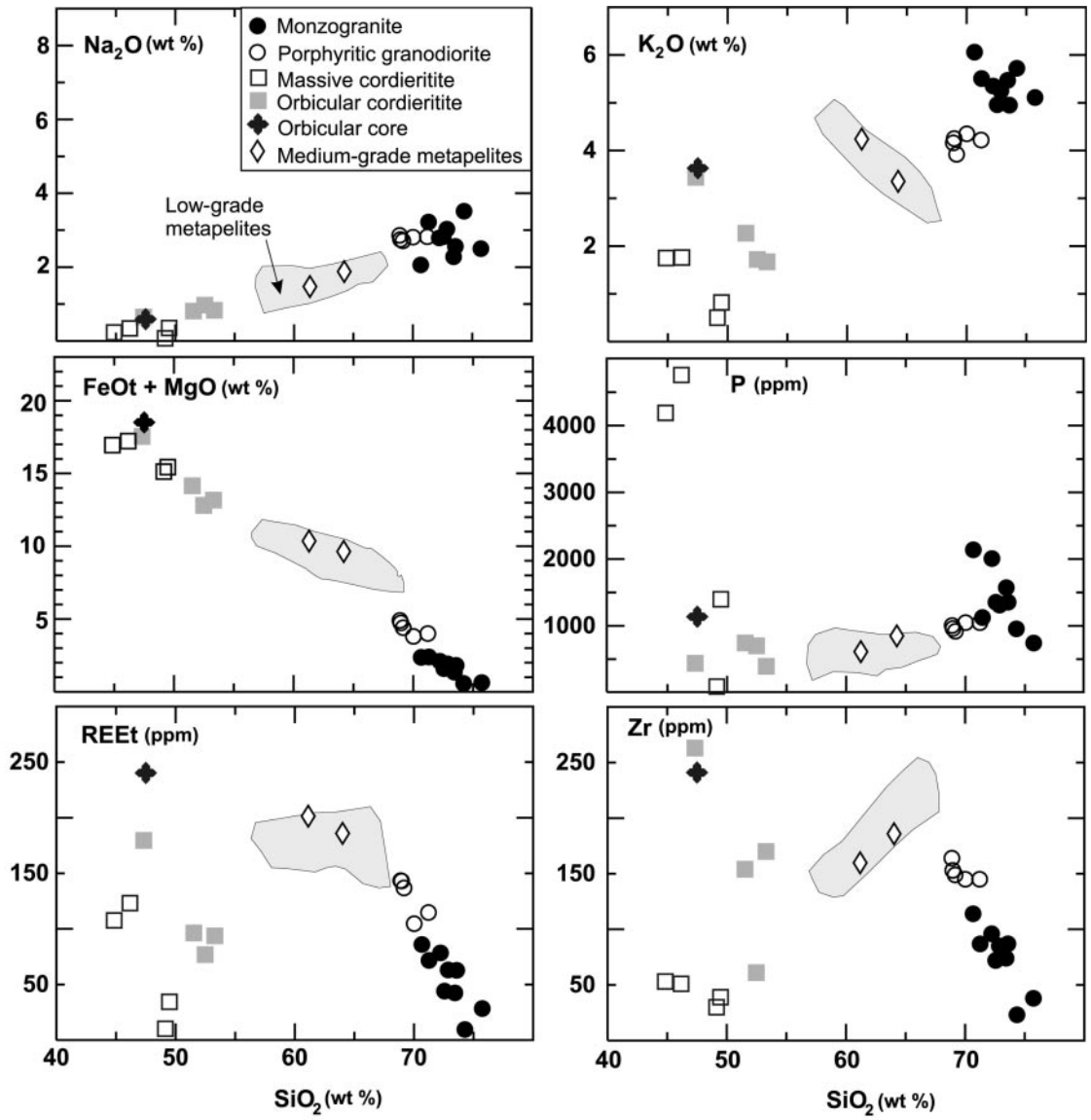

Fig. 8. Selected major and trace element Harker variation diagrams for granitoid and metamorphic rocks of the El Pilón complex. Samples of medium-grade metapelitic schists are from large outcrops located 15 km to the NW of the complex (see Fig. 1).

is that metapelites with 57–67% SiO_2 plot in an intermediate position between the cordieritites and the granites.

The porphyritic granodiorite of El Pilón is characterized by SiO_2 = 69–71%, ASI = 1·26–1·38, Na_2O + K_2O = 6·7–7·2%, *mg*-number = 46–49, K/Rb = 180–220, REEt (total rare earth elements) = 110–150 ppm, $[La/Yb]_N$ = 7·5–10·5 and Eu/Eu* = 0·52–0·63. The monzogranitic pluton associated with the cordieritites has a more evolved chemistry, and is distinguished by a high K_2O/Na_2O ratio (1·7–3·0) and high P_2O_5 content (0·2–0·5%). The normal facies in the central part of the pluton has SiO_2 = 70·7–73·6%, ASI = 1·23–1·34, Na_2O + K_2O = 7·4–8·2%, FeO + MgO = 1·4–2·4, *mg*-number = 25–45, K/Rb = 185–240, REEt = 43–87 ppm, $[La/Yb]_N$ = 4–5·5 and Eu/Eu* = 0·42–0·63. However, local monzogranites in association with the Cerro Negro and Tamaín cordieritite bodies are more leucocratic (FeO + MgO = 0·5–1·5%, SiO_2 = 73·5–75·7%), and are characterized by depleted REE patterns with positive Eu anomalies (REEt = 8–28 ppm, Eu/Eu* = 1·4–3·5, Figs 9–11). Compared with typical felsic crustal granites such as the Himalayan and Hercynian leucogranites, the highly peraluminous monzogranites of El Pilón are depleted in Na_2O, enriched in K_2O and show distinctively high K/Rb ratios (Fig. 9). In

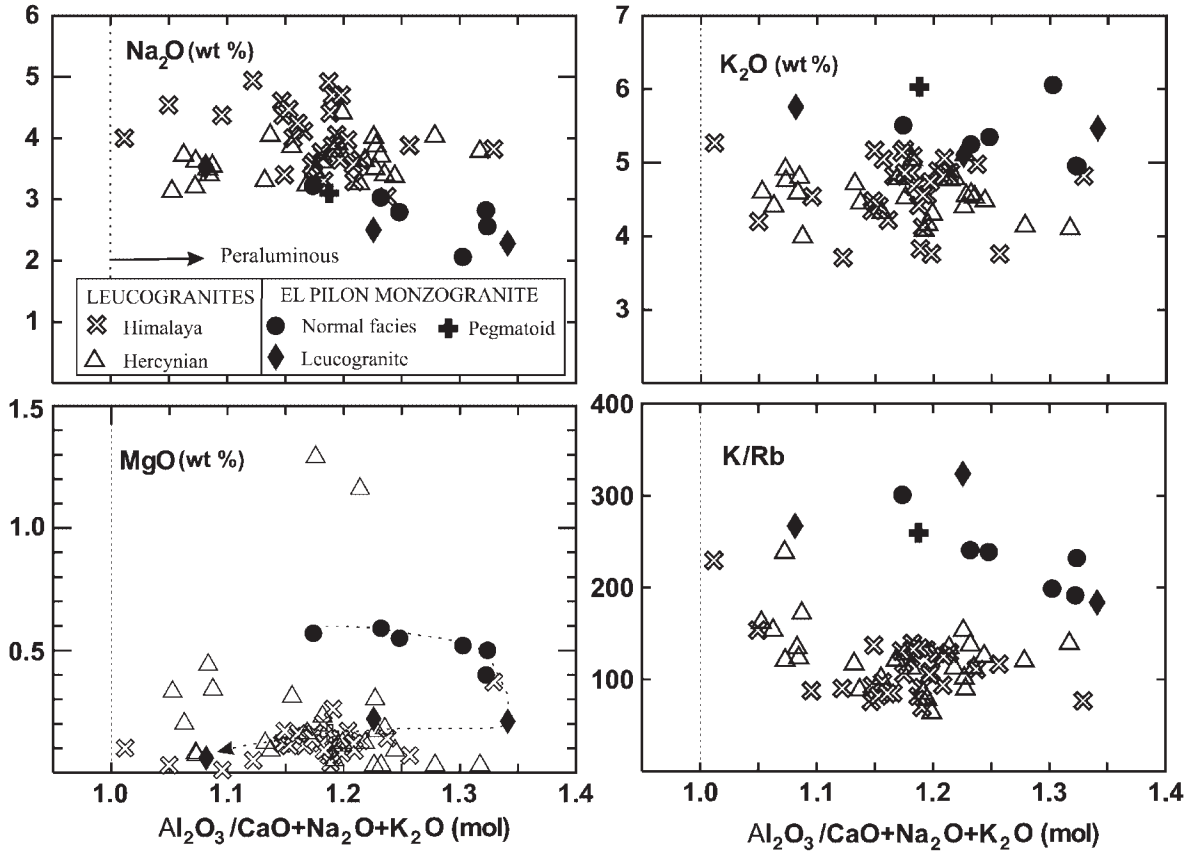

Fig. 9. Alumina saturation index (ASI = mol. $Al_2O_3/CaO + Na_2O + K_2O$) vs Na_2O, K_2O, MgO and K/Rb for El Pilón, Himalayan and Hercynian granites. Data sources: Dietrich & Gansser (1981), Le Fort *et al.* (1987), Crawford & Windley (1990) and Scaillet *et al.* (1990) for Himalayan leucogranites; Willamson *et al.* (1996), Villaseca *et al.* (1998*b*) and C. Villaseca (unpublished data, 2000) for Hercynian leucogranites from the Massif Central, France, and the Central System, Spain.

the normative plot Qtz–Ab–Or (not shown) the granites of El Pilón plot near the low-pressure cotectic, but displaced from the H_2O-saturated minima at 1–2 kbar towards the Qtz–Or side.

Cordierite- and tourmaline-bearing pegmatoids associated with the monzogranite form a more heterogeneous granitoid group, with SiO_2 = 67·75–73%, ASI = 1·19–1·21, $Na_2O + K_2O$ = 9·1–9·2%, *mg*-number = 30–40, K/Rb = 130–250, REEt = 10–22 ppm, $[La/Yb]_N$ = 2·5–3·5 and Eu/Eu* = 1·2–1·4. Flat REE patterns with positive Eu anomaly are distinctive (Fig. 11).

The cordieritites are distinguished from pure cordierites by high K_2O and low Al_2O_3, as a result of the variable but ubiquitous presence of modal biotite. The massive cordieritite approaches the composition of pure cordierite (SiO_2 = 45–59%, FeO_t + MgO = 15–17%, K_2O = 0·5–1·7%, *mg*-number = 61–67, REEt = 10–130 ppm, $[La/Yb]_N$ = 1·5–3, Eu/Eu* = 0·15–0·9). Schreyer *et al.* (1979) reported the occurrence of a Na–Be cordierite (*mg*-number = 62, BeO = 0·93%, Na_2O = 1·25%), but this is outside the typical range of Na_2O = 0·25–0·49% that we have found in our new microprobe analyses of the different facies of the cordieritites. The whole-rock compositions of some orbicular cordieritites from Cerro Negro have high SiO_2 and Na_2O, reflecting the minor modal quartz and plagioclase observed in their restitic cores (Fig. 8). Trace elements such as Rb, REE and Zr are also enriched in the orbicule cores, either because they occur mainly in accessory minerals (apatite, or zircon armoured in biotite), or as a result of replacement in biotite of K by Rb. The restitic orbicular nucleus is characterized by SiO_2 = 47·5%, FeO_t + MgO = 18·5%, K_2O = 3·6%, *mg*-number = 53·6, K/Rb = 195, REEt = 253 ppm, $[La/Yb]_N$ = 10·6 and Eu/Eu* = 0·27.

Sr AND Nd ISOTOPE DATA

Rapela *et al.* (1998*b*) presented Rb–Sr analyses of the massive cordieritite, the biotite + sillimanite orbicular

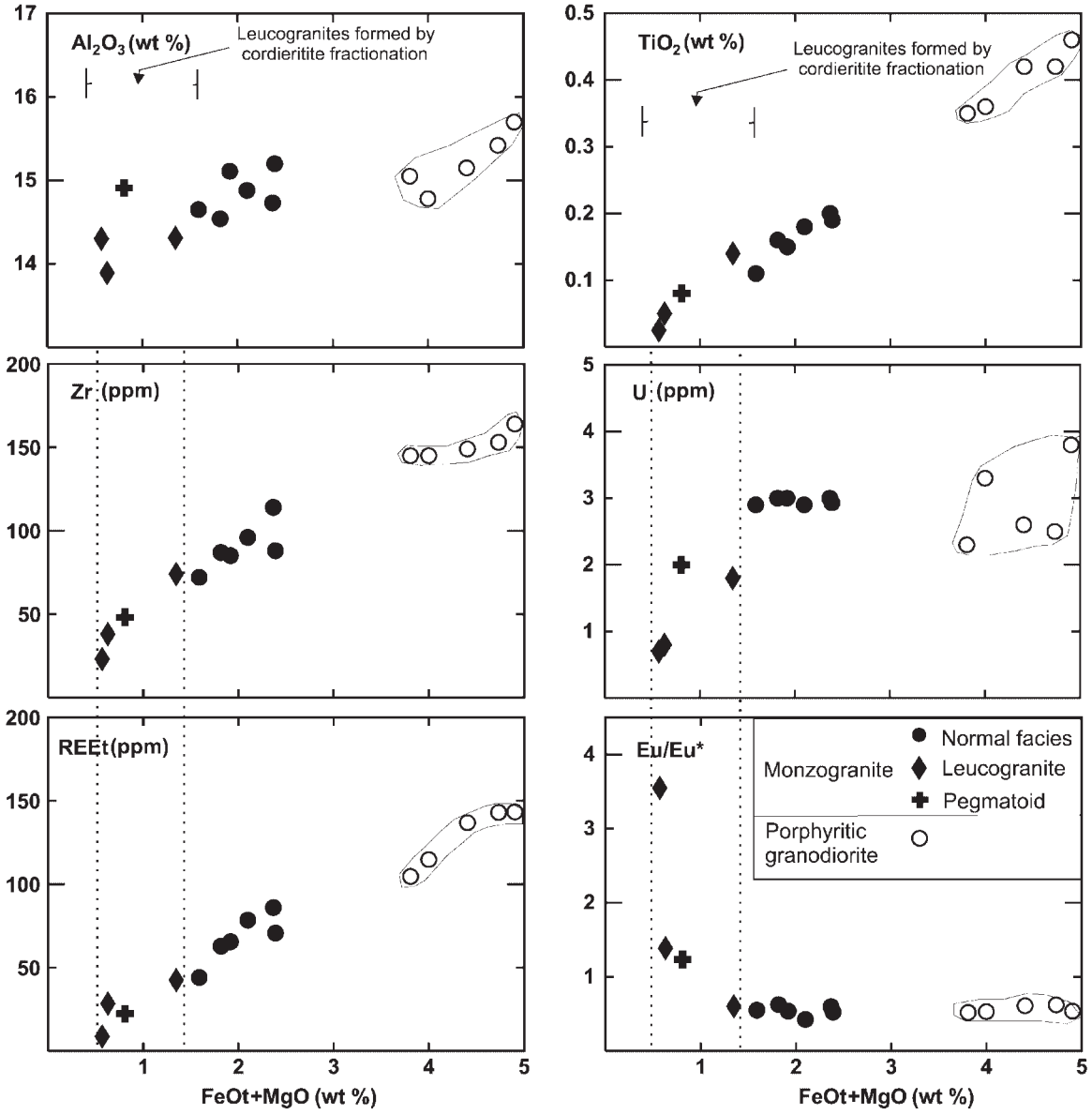

Fig. 10. FeO_t + MgO vs Al_2O_3, TiO_2, Zr, U, REEt and Eu/Eu* for the granitoid units of El Pilón complex. The sharp decrease in U, Zr and REEt, and the development of positive Eu anomalies in the leucogranites are produced by apatite and zircon fractionation armoured in cordierite and restitic clusters of Bt + Sil.

nuclei and the leucogranite and pegmatitic facies that defined a Rb–Sr isochron corresponding to 523 ± 4 Ma [mean square weighted deviation (MSWD) = 2·3, n = 18]. Together with the uniform initial $^{87}Sr/^{86}Sr$ of 0·7136 ± 0·0005, this is taken to demonstrate that all these rock-types were coeval and genetically linked. Moreover, the Rb–Sr age is concordant with the U–Pb zircon age of 523 ± 2 Ma obtained from the main porphyritic granodiorite, demonstrating that all facies of El Pilón complex were emplaced during the same Early Cambrian episode. The initial $^{87}Sr/^{86}Sr$ of the porphyritic granodiorite is, however, slightly lower: the weighted mean for six samples of Rapela *et al.* (1998*b*), calculated at 523 Ma, is 0·7126 ± 0·0005. Nevertheless, both values are within the ranges for the high-grade migmatites and gneisses of the Sierras de Córdoba (0·7137–0·7165) and for the low- to medium-grade schists and phyllites (0·7109–0·7163), both calculated at 530 Ma (Rapela *et al.*, 1998*b*). It is clear that the magmatic rocks of the El Pilón complex have been derived from sources comparable with these

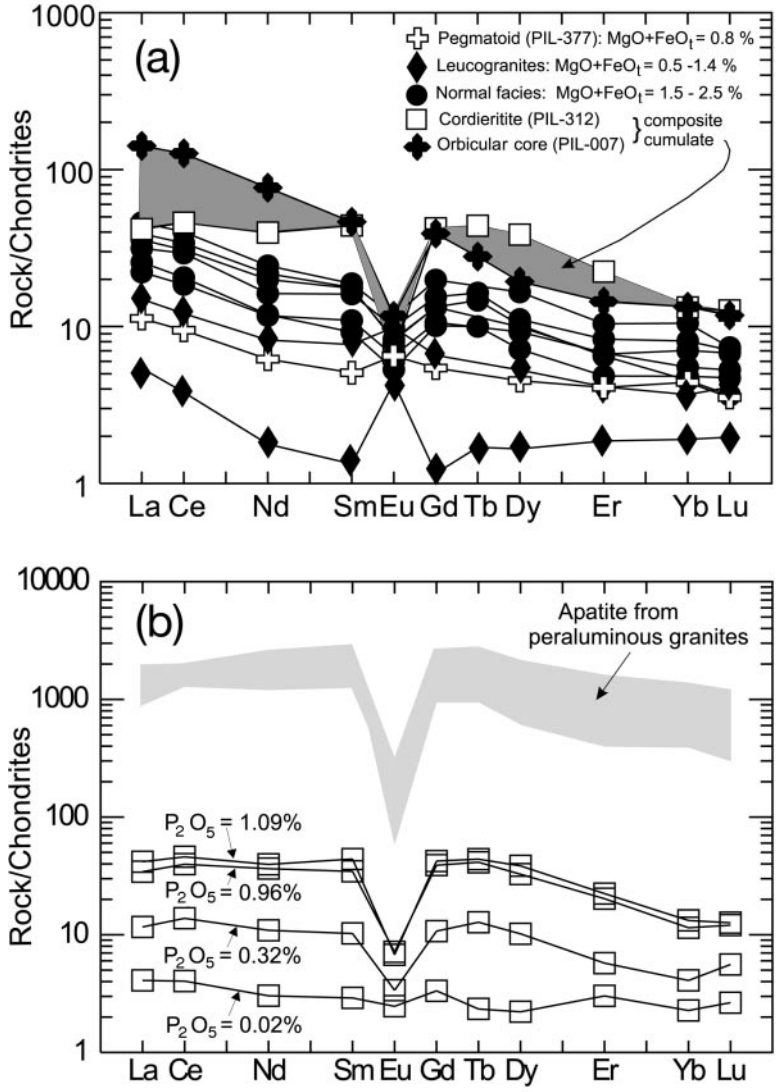

Fig. 11. (a) Representative REE patterns of the monzogranite, the massive cordieritite and the orbicular core. (b) REE pattern of the massive cordieritites showing the increase in total REE and negative Eu anomaly with increasing P_2O_5 content. The field for apatite in peraluminous granites is from Bea (1996).

local crustal metamorphic rocks, or at least that they incorporated a substantial component from them.

A more detailed isotopic treatment of the petrogenetic relationships is not possible with Rb–Sr data, as the highly peraluminous granites and, especially, the cordieritites have very high Rb/Sr ratios, leading to significant errors in the calculation of Sr-isotope compositions in Cambrian times. Moreover, the mobility of these elements in fluid-present systems is well known and leads to uncertainty in interpretations. We prefer therefore to rely on more robust Sm–Nd data and have more than doubled the number of samples analysed by Rapela *et al.* (1998*b*), including some duplicate analyses. These data are presented in Appendix 3 (available from the *Journal of Petrology* Web site) and the initial compositions are displayed graphically in Fig. 12.

The εNd_{523} values of the monzogranite, pegmatites, restite and massive cordieritites are very consistent ($-5{\cdot}5$ to $-6{\cdot}7$, mean of 16 values $-6{\cdot}1 \pm 0{\cdot}2$), indicating attainment of a high degree of isotopic equilibrium during the melt segregation process. The values for the country rocks are more variable, as might be expected, reflecting considerable inhomogeneity at 523 Ma ($-3{\cdot}0$ to $-7{\cdot}8$). If the few extreme values above $-3{\cdot}0$ and below $-7{\cdot}0$ are excluded, the high-grade gneisses have a mean of $-5{\cdot}4 \pm 0{\cdot}7$, and the low- to medium-grade schists and phyllites a mean of $-6{\cdot}5 \pm 0{\cdot}9$. Thus both could have contributed to the anatectic melt that formed the

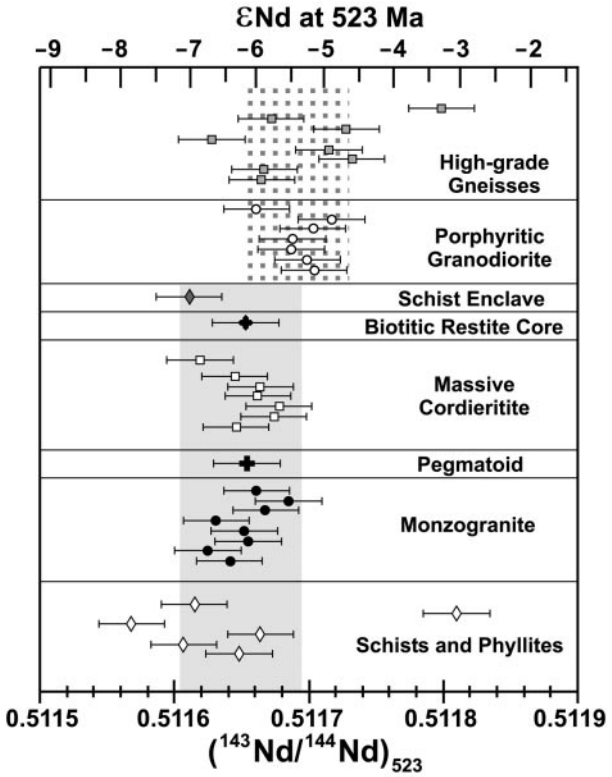

Fig. 12. Plots of initial Nd isotope compositions for samples from the El Pilón complex and country rocks. The shaded and dotted columns represent the effectively different compositions of the monzogranite (closely similar to the phyllites and low-grade schists), and the porphyritic granodiorite (more similar to the high-grade country rocks), respectively.

monzogranite magma. Seven analyses of the porphyritic granodiorite give a mean εNd_{523} value of $-5{\cdot}3 \pm 0{\cdot}3$, indistinguishable from that of the high-grade gneisses and confirming the impression obtained from the Sr data that its source was slightly more primitive in terms of isotopic evolution than that of the monzogranite–cordieritite–restite association. Crust-derived Sm–Nd model ages (De Paolo *et al.*, 1991) of all rocks of the El Pilón complex are consistently Mesoproterozoic; averaging $\sim$1700 Ma for the highly peraluminous association and the schists, and $\sim$1650 Ma for the porphyritic granodiorite and the gneisses. Interpretation of these observations in terms of the magmatic history is considered more fully below.

DISCUSSION

Geological environment of the cordieritites

The high dT/dP gradient of the Middle Cambrian M_2 metamorphism during which the cordieritites and highly peraluminous granites of El Pilón were emplaced has been ascribed to (1) isothermal uplift following crustal thickening, ophiolite obduction, compression and high-grade metamorphism (Rapela *et al.*, 1998*a*) or (2) ridge subduction under the accretionary prism (Fantini *et al.*, 1998). Orbicular cordieritites similar to the well-preserved facies of Cerro Negro are extremely rare. To our knowledge, the only other described example of orbicular cordieritite is that of Minedera-yama, Tsukuba, Japan, consisting of ellipsoidal orbicules with cordierite shells and schistose biotite–plagioclase cores set in a granular granitic matrix (Kawano, 1933; Yoshiki, 1933). The field association with porphyritic granites, the fabric of the orbicular rock, the mineralogy (including abundant accessory apatite), and the chemical composition, all resemble features of El Pilón. In Minedera-yama the orbicular cordieritite occurs as a dyke in a porphyritic biotite granodiorite–monzogranite of Latest Cretaceous–early Palaeogene age (59–63 Ma), which intrudes a low P/T shale and sandstone sequence considered to be an eastern extension of the Ryoke metamorphic belt of SW Japan (S. Ishihara, personal communication, 2000). A tectonic model for the Ryoke belt involving ridge subduction followed by terrane amalgamation of the high-P/T rocks of the Sanbagawa belt has been recently proposed (Brown, 1998).

The cordierite–sillimanite-bearing granitic rocks of El Pilón also show many similarities with widespread granitic massifs formed during the late thermal evolution of the Hercynian domain in western Europe and northwestern Africa (Gardien *et al.*, 1997; Escuder Viruete *et al.*, 1998). Central Iberian massive cordieritites with 60–80% cordierite have been related to assimilation of restitic metasedimentary material by the granitic magmas (Ugidos, 1988; Ugidos & Recio, 1993). A high-level pluton in Morocco contains cordieritite enclaves (80% Crd) inferred to be partly digested pelitic xenoliths picked up by the ascending magma (Bouloton, 1992). Another well-studied example of these low-P, high-T terranes associated with highly peraluminous cordierite-bearing granites is the Velay dome in the French Massif Central (Barbey *et al.*, 1999, and references therein), although no cordieritites have been found in this case. The high dT/dP gradient in the Velay dome cannot be explained by post-tectonic uplift alone as deduced from calculated uplift rates, but several lines of evidence suggest heat supplied by hot mantle-derived magmas at the base of the crust during the extensional D_4 deformation phase (Montel *et al.*, 1992). The El Pilón peraluminous granites show no evidence of coeval mantle-derived rocks, but Cambrian uplift rates have not been yet accurately estimated in the Sierras de Córdoba, and therefore underplating by mafic magmas during the later stages of the M_2 event cannot be ruled out. The common environmental links between the cordieritites of El Pilón, Minedera-yama and the Hercynian belt are the high dT/dP metamorphic gradient and an association with peraluminous granites containing

fertile pelitic enclaves. The orbicular cordieritites of El Pilón and Minedera-yama appear to be closely related to dykes or conduits. Despite this general coincidence in the geological environment, cordieritites are scarce even in large low-*P*, high-*T* domains such as the Velay dome. This indicates that other local factors such as availability of sufficient water to allow local fluid-present melting of metapelites, high temperatures, and cordierite accumulation by flow segregation, are needed to form relatively large cordieritite outcrops such as in El Pilón (see below).

Cordieritites are not restricted to the localities mentioned above, and the following examples, not intended as a thorough compilation, illustrate the scattered occurrence of cordierite-rich rocks in orogenic belts of different ages and continents, although in some cases the modern petrological studies are lacking. Read (1923, 1935) first described cordierite-rich rocks of igneous aspect from the Dalradian Series of NE Scotland, the classic area for 'Buchan type' low-*P* (1–3 kbar), high-*T* (500–550°C) regional metamorphism, analogous to the Ryoke belt of Japan. Massive layered gabbros were emplaced at, or soon after, the peak of metamorphism, and are associated with quartz–cordierite norites and quartz–cordierite–garnet–feldspar rocks with cordierite up to 20–35% of the mode, both containing metapelitic xenoliths. Petrological arguments, field relations, and isotopic data are consistent with melting of the host pelitic schists in the roof zone of the gabbros (Gribble & O'Hara, 1967; Gribble, 1968; Pankhurst, 1969). Mathias (1952) described and analysed an 'unusual' rock, composed of 63% of porphyroblastic cordierite, associated with granites at Upington, South Africa, that are most probably part of the 1000–1200 Ma Namaqualand metamorphic complex (R. Armstrong, personal communication, 2000). In the Strathbogie batholith, a subvolcanic S-type body of the Lachlan Fold Belt (Phillips *et al.*, 1981), a cumulate layer probably formed by a flow segregation is found near the edge of a pluton lobe. This contains ~30% euhedral cordierite, biotite booklets, plagioclase, a little interstitial quartz and relatively high concentration of the usual accessory minerals (J. D. Clemens, personal communication, 2000).

Magma sources and ascent mechanism of El Pilón magmas

The highly peraluminous mineralogy and geochemistry of these granites, coupled with the radiogenic Sr and unradiogenic Nd isotopic signatures, demonstrate major involvement of a mature metasedimentary component in their source (Figs 3 and 12). The mid-crustal high-grade Grt + Crd migmatitic massifs of the Sierras de Córdoba, formed during the M_2 metamorphic peak (Rapela *et al.*, 1998*a*; Otamendi *et al.*, 1999), are an obvious potential candidate for this source. The protolith of the high-grade rocks is inferred to be Bt + Grt gneisses derived from metaluminous greywackes with SiO_2 = 69·8–72·5%, Al_2O_3 = 12·0–13·6%, MgO = 2·2–2·7%, K_2O = 2·0–2·6% and Na_2O = 2·0–2·6%, with very little if any shale intercalations (Otamendi & Patiño Douce, 2001). It is very likely that such high-grade rocks underlie the lower-pressure Crd migmatites that host the El Pilón complex. The presence or absence of garnet is the only difference between these two types of migmatite, which are separated by a ductile shear zone to the east of El Pilón (Fig. 1). Another potential metasedimentary source is the low- to medium-grade phyllites and schists of the Sierras de Córdoba, and equivalent Cambrian supracrustal sequences in other parts of the Sierras Pampeanas (Rapela *et al.*, 1998*a*; Pankhurst *et al.*, 2000). Schists cropping out to the NE of El Pilón, and abundant enclaves in the monzogranite, are representative of this sequence, in which metapelite protoliths commonly contain 57–67% SiO_2, 14·2–19·0% Al_2O_3, 2·6–5·3% MgO, 2·6–5·0% K_2O and 0·6–2·2% Na_2O (Fig. 8). Initial Sr and Nd isotope ratios indicate that the garnet-bearing, high-grade metasedimentary rocks are slightly but consistently less evolved isotopically than the low- to medium-grade rocks (Fig. 12). This shows that the protoliths of the two metamorphic sequences are not identical in composition. The porphyritic granodiorite of the El Pilón complex has isotopic compositions similar to those in the high-grade rocks. In contrast, the monzogranite is isotopically more evolved and displays a range of initial ratios transitional to the field of low- to medium-grade metamorphic rocks (Fig. 12). This, and the large number of schist enclaves found in both the monzogranite and the cordieritites, is consistent with an important contribution from a relatively mature metasedimentary source similar to the low- to medium-grade regional schists and phyllites.

On the other hand, the abundant Grt + Bt enclaves in both the porphyritic granodiorite and the monzogranite show that, although contaminated at emplacement level by *in situ* segregations and/or assimilation of garnet-absent host rocks, the primary source of the peraluminous magmas was located at a deeper level. The pressure of 5·9 kbar calculated from the core of a restitic garnet in the cordieritite (Figs 6 and 7) is taken as an indication of the depth of the magma sources. This is consistent with coeval generation of extensive migmatitic massifs at the same depth during the thermal peak of the M_2 metamorphism in the Sierras de Córdoba, dated at 522 ± 8 Ma (Rapela *et al.*, 1998*b*). Vertical migration through ~6–8 km is implied if a melt segregated from a magmatic source at ~6 kbar was finally emplaced at 3·5–4 kbar. Peak *P–T* condition estimations in Crd + Grt migmatitic massifs of the Sierras de Córdoba formed during the M_2 episode decrease towards the north (Fig. 7), suggesting

exposure of progressively higher levels of the Cambrian crust, at which peraluminous magmas started to accumulate. On the basis of the field relations of the monzogranite and cordieritite, and the illustrative cross-sections (Fig. 2), we argue that the monzogranite melt migrated by a dyke mechanism (e.g. Clemens, 1998; Petford *et al.*, 2000, and references therein), and that cordieritites were locally formed at the top ends of feeder conduits during the laccolithic emplacement of the monzogranite body. Given the small size of El Pilón monzogranite, emplacement in <100 years may be inferred from the estimated filling times for tabular disc-shaped plutons (Petford *et al.*, 2000, fig. 4). Consequently, the time interval between the P–T conditions inferred for magmatic segregation and the lower pressure re-adjustment registered in the restitic association of the cordieritites (Figs 6 and 7) was probably of the same order of magnitude. This is consistent with the fact that the ages of the granites and migmatites are indistinguishable, and implies extremely rapid ascent of the highly peraluminous melts at the start of the decompression stage of the Pampean orogen in the Sierras de Córdoba.

From the Cerro Negro and Tamaín conduits the monzogranite melt extended laterally over the porphyritic granodiorite forming two interconnected subcircular granitic lenses. The three-dimensional shape of this small-scale laccolith resembles the 'pinch and swell' type geometry of multiple laccolith formation in the Himalayas, which may represent a common emplacement mechanism in extending collisional belts (Scaillet *et al.*, 1995*a*). As in the Himalayan laccoliths, the two-lens boudin geometry of the El Pilón monzogranite seems to be more obviously related to melt supply from two different conduit feeders (Cerro Negro and Tamaín, Fig. 2), rather than to regional deformation. Recognition of feeder dykes is difficult, so that the association of orbicular facies and conduit feeders found at El Pilón might be profitably sought in large batholiths, where the orbicular facies are usually restricted to structural traps into which upward-migrating solute-rich water was channelled (e.g. the Sierra Nevada batholith, Moore & Lockwood, 1973).

Both the monzogranite and the porphyritic granodiorite were emplaced at or near the contact between the Crd migmatites and the schists. This limit, located at $\sim$3·5–4 kbar, represented an important subhorizontal anisotropy in the crustal section at El Pilón; peraluminous granites formed during the anatectic stage were not emplaced in the phyllites and low-grade schists above this level. An exposure of medium-grade schist with Crd porphyroblasts 14 km from the complex suggests that the emplacement of peraluminous plutons beneath the schist unit extended to this distance. During extensional regional stress, magma driving pressure may greatly exceed the lithostatic load, resulting in subhorizontal sheet-like intrusions (Hogan *et al.*, 1998). In the case of El Pilón complex, the boundary between two different metasedimentary units seems to have behaved as an effective magma trap.

Compared with the monzogranite, there is no field evidence from which to infer a feeder-like mechanism for emplacement of the porphyritic granodiorite, as the floor of the pluton is not exposed. Nevertheless, as for the monzogranite, garnet–biotite restitic enclaves in the granodiorite indicate that the source of the melt was at least 6 km below the intrusion level, and U–Pb and Rb–Sr geochronological data indicate that both units were intruded during the same event (Rapela *et al.*, 1998*b*). We argue that the absence of thermal contrast between the granodiorite and the country rock may reflect thermal equilibrium between a large batch of accumulated melt and the metamorphic envelope at 3·7 kbar. A slow ascent mechanism, such as diapirism, for the granodiorite pluton and a fast feeder emplacement for the monzogranite are mutually exclusive. If the ascent of the porphyritic granodiorite was by feeder-dyke mechanism similar to that for the monzogranite, the rapid intrusion of large amounts of hot highly peraluminous magmas into the upper crust would have been critical in developing the high dT/dP gradient during the later stages of the M_2 metamorphism. We suggest that it triggered widespread partial melting and led to formation of cordierite-bearing migmatites, which also acted as a rheological screen.

Partial melting and the role of fluids at the emplacement level

The remarkably fresh and well-developed orbicular cordieritites of Cerro Negro share many, if not all, of the features of fabric, rheological behaviour and setting with the orbicular granite facies (Elliston, 1984). An important characteristic common to many orbicular granites is their restriction to small lenses, pipes and water-rich marginal facies of the magma from which they crystallized (Elliston, 1984). Their development seems to require an absence of nuclei in the magma accompanied by a fall in the liquidus temperature of the melt, forcing crystallization to occur only on solid objects (Vernon, 1985). An effective way to cause a drop in the liquidus temperature of an H_2O-undersaturated magma is by introduction of H_2O into the melt (Vernon, 1985). At El Pilón, the local concurrence of cordieritites, tourmaline-bearing pegmatoids and hydrothermal alteration is consistent with intense fluid activity associated with the feeder conduits represented by the cordieritite pipes. Nevertheless, the most likely source of the highly peraluminous granites of El Pilón is Grt + Crd migmatites formed at $\sim$6 kbar.

The peraluminous magmas of the Sierras de Córdoba are H_2O-undersaturated melts formed by partial melting,

either in the presence of a small amount of free water (H_2O-fluxed melting) or by dehydration melting of biotite (Otamendi & Patiño Douce, 2001). The initial temperature of the monzogranite melt at the emplacement level has been inferred from the temperatures estimated for the source (5·9 kbar, 780°C), and by assuming an ascent path with a constant and very low crystal/melt ratio. This steep path is akin to those followed by melts that remain isothermal and H_2O undersaturated, with a minimal chemical and thermal exchange between magma and country rocks, as in dyke ascent (dashed line in Fig. 7; Johannes & Holtz, 1996; Petford *et al.*, 2000). A very slight fall in temperature of ~10°C is inferred for the ascent of a melt from 5·9 kbar to the emplacement level at 3·7 kbar. Taking the temperature of Paragenesis 2 in the cordieritite (PIL-375, 650°C) as representative of the final temperature after isobaric cooling, this yields a crystallization interval of ~110°C (Fig. 7). This interval is consistent with those observed for peraluminous leucogranites under water-saturated conditions at 4 kbar (70–120°C), which increase with decreasing aH_2O (Scaillet *et al.*, 1995*b*). The initial temperature of ~770°C inferred for the water-undersaturated peraluminous melt is within the range of liquidus temperature for Bt + Ms leucogranites at 4 kbar with H_2O_{melt} >5% (770–800°C, Scaillet *et al.*, 1995*b*), and is well above that of the relict St + Bt1 + Ms1 association observed in the pelitic schists close to the El Pilón complex (Fig. 1, Table 1). The abundant restites of assimilated schists, including those at the core of the orbicular cordieritite and the poikilitic Crd–Bt2–Ms2 association developed in the schists to the NE of the complex, indicate that significant thermal disequilibrium must have initially existed at the magma emplacement level.

Ascending magmas with constant crystal/melt ratio produce an increase in aH_2O with decreasing pressure (Johannes & Holtz, 1996), which in the case of El Pilón complex would have been accentuated at the top of the feeder conduits as a result of water released by partial melting of the hydrous country rock schists. The schists contain 16·3–18·1% Al_2O_3, 3·2–3·4% MgO and ~2 wt% H_2O^+ (see Appendix 1), whereas the probable unmelted source rocks are biotite–garnet gneisses with 12·0–13·6% Al_2O_3 and 2·2–2·7% MgO (see Table 2; Otamendi & Patiño Douce, 2001). Water-saturated melting experiments on peraluminous rocks at 2–5 kbar have shown that the amount of cordierite formed increases with increasing Al_2O_3 excess at constant pressure, whereas the stability field of biotite decreases as a result of preferential partitioning of Mg into cordierite (Puziewicz & Johannes, 1988). This is relevant for the El Pilón case, as fluid-present melting of the pelitic schist enclaves leaving garnet-absent Bt–Sil restites at 3·5–4 kbar would have increased the Al, K, P, Fe and Mg contents and *mg*-number in the melt ($mg\text{-number}_{biotite}$ = 49–56). Although the solubilities of ferromagnesian components in H_2O-undersaturated felsic melts are very low (e.g. Johannes & Holtz, 1996), at constant temperature and pressure MgO and FeO concentrations in granitoid melts vary directly with H_2O content (Patiño Douce, 1996, and references therein). Ca-poor peraluminous melts incorporate up to 0·6–0·7% MgO, in contrast to ≤0·15% MgO in subaluminous melts, which also have significantly lower Mg/Fe ratios (Holtz *et al.*, 1992). The normal facies of the monzogranite contains 0·4–0·6% MgO and has very high ASI compared with Hercynian and Himalayan granites (Fig. 9). Early crystallizing cordierite from this melt would therefore be expected to have a high *mg*-number, suggesting that the massive cordierite (*mg*-number = 65–70) started to crystallize in the fluid-rich environment associated with the cordieritite pipes, when the melt became saturated in MgO. An early crystallizing high-Mg cordierite is in accord with experimental evidence indicating that some Al forms complexes with Mg in Mg-bearing highly peraluminous melts (Holtz *et al.*, 1992).

Provided that equilibrium were attained in the partial melting of schists at the emplacement level, a melt with a high K/Rb ratio would be expected, as biotite was the main rock-forming mineral in the residue and the $Kd^{biotite/melt}$ for Rb is very high. Fluid-present partial melting of hydrous country rocks near magma conduits provides a suitable model to explain the massive occurrence of magmatic cordierite in very restricted environments, as well as the high MgO content, high ASI, and high K/Rb ratio of the consanguineous melts (Fig. 9).

Even without reaching H_2O saturation, an increase in the H_2O and fluid content of the highly peraluminous melt as a result of rapid decompression and partial melting of hydrous Al-rich country rocks may have produced an important drop in the liquidus temperature and changes in the composition of the magma. Another consequence of fluid-present melting is depression of the Pl + Qtz solidus, so that residues formed by H_2O-fluxed melting contain significantly less plagioclase (and quartz) than those formed by dehydration melting (Patiño Douce & Harris, 1998). Hence, with preferential partition of quartz and feldspar into melt, biotite-rich residues are expected to be a common product of medium- to low-pressure, fluid-present melting of biotite-bearing metasedimentary rocks. Mass balance calculations between the low- and medium-grade metapelites (see the compositional field of these rocks in Figs 3 and 8) and the normal facies of the monzogranite indicate that residues with a silica composition akin to that of the restitic core of the orbicule (sample PIL-007) would be achieved if the melt fraction were at least 50–60% (Table 2a). Although the quantitative

Table 2: Mass balance calculations

(a) Calculated residues after 40–60% extraction of monzogranite from average metapelite

(wt %)	Average metapelite	Average monzogranite	Calculated residues			Observed residue (PIL-007)
			40%	50%	60%	
SiO_2	61·50	72·37	54·25	50·63	45·20	47·51
TiO_2	0·80	0·16	1·23	1·44	1·76	1·53
Al_2O_3	18·00	14·77	20·15	21·23	22·85	25·62
FeO(t)	6·50	1·45	9·87	11·55	14·08	11·23
MnO	0·09	0·04	0·12	0·14	0·17	0·26
MgO	3·15	0·48	4·93	5·82	7·16	7·28
CaO	0·95	0·76	1·08	1·14	1·24	0·31
Na_2O	1·55	2·68	0·80	0·42	−0·15	0·59
K_2O	4·10	5·36	3·26	2·84	2·21	3·63
P_2O_5	0·16	0·35	0·03	−0·03	−0·13	0·26
Total	96·8	98·42	95·72	95·18	94·37	98·22

(b) Least-squares fractionation model for monzogranite and cordieritite

(wt %)	Parental magma (average monzogranite)	Fractionated magma (average leucogranite)	Composite cumulate PIL-303 (cordieritite)	Difference obs.–calc. parent (wt %)
SiO_2	72·37	75·00	47·33	0·02
TiO_2	0·16	0·04	0·21	0·11
Al_2O_3	14·77	14·01	25·49	−0·05
FeO(t)	1·45	0·46	10·37	0·19
MnO	0·04	0·01	0·21	0·01
MgO	0·48	0·14	7·17	−0·24
CaO	0·76	0·79	0·14	0·03
Na_2O	2·68	3·02	0·65	−0·13
K_2O	5·36	5·58	3·44	−0·01
P_2O_5	0·35	0·20	0·10	0·16
Total	98·42	99·25	95·11	

Sum of square of residuals = 0·150; percent of cumulate assemblage = 7·9%.

comparison is limited by unmeasured variations in the modal proportions of Bt, Sill and Crd in the core of the orbicules, the high colour index and concentration of refractory minerals observed in most cores (see Fig. 4) indicate a high degree of partial melting of the schist enclaves. Negative values of P_2O_5 and CaO for calculated residues at 50–60% melting (Table 2a) are related to the preferential partition of apatite in the cordieritites and highly peraluminous melts subsequently formed (see Fig. 11 and below). Melts produced by anatexis of the metapelitic enclaves mixed at the final emplacement level of the body with the monzogranitic melts formed at greater depth in the garnet stability field. Such strong upper-crustal contamination may have not significantly changed the highly peraluminous chemistry of the magma, as a metasedimentary source was probably involved at depth. However, the more evolved Sr and Nd isotopic compositions of the

monzogranite clearly indicate the influence of an evolved crustal component, such as the low- and medium-grade rocks of the Sierras de Córdoba (Fig. 12).

Orbicular cordieritite: an *in situ* cumulate rock formed from highly peraluminous melts

The zoning and radial arrangement of cordierite crystals that decrease in size towards the outer edge of the shells of the large orbicules suggests static growth in a liquid environment (Fig. 4). There is no genetic difference between this cordierite and that of the massive variety, as cordierite crystallized from magma on any available solid object: (1) Sil + Bt schist restites; (2) euhedral first-formed crystals of cordierite; or (3) the sides of the conduits and/or the magma chamber. Crystallization types (1) and (2) led to formation of orbicular cordieritite whereas crystallization type (3) developed the massive variety. Crystallizing directly from the magma under fluid-present conditions, the cordierite of the cordieritites is a magmatic mineral growing in a environment close to that found in pegmatitic systems (Clarke, 1995). Melt supply through the feeder conduits was probably pulsed or intermittent, as inferred from the fabric of the orbicular cordieritite. The static growth of large orbicules during the initial stage of crystallization of the monzogranitic magma was followed by periods of transport, accumulation and deformation of the orbicules at the funnel-shaped end of the feeder dyke. Breccia facies, angular enclaves and disrupted outcrops associated with the massive cordieritites also reflect rapid and turbulent flow, probably produced by a sudden release of pressure during the filling of the laccolith by a fluid-rich melt. The decreasing size of the orbicules towards the top of the Cerro Negro section suggests that flow segregation along the upper section of the feeder conduit produced a magmatic analogue of graded bedding in sedimentary rocks (Fig. 2).

The leucogranitic orbicular matrix, which is transitional to the local facies of the monzogranite, is interpreted as a solidified remnant of the magma from which the orbicules crystallized. Initial Sr and Nd ratios of the orbicule cores, the massive cordieritite and the monzogranite are all indistinguishable, indicating that near isotopic equilibrium was attained during the crystallization of the orbicules at high temperature (Fig. 12). This remarkable isotopic homogeneity for a melt derived from a heterogeneous sedimentary source can only be explained by effective mixing of the melt after the emplacement and contamination by *in situ* partial melting of metapelitic enclaves. Effective mixing is best explained by strong convection within the laccolith body. Thus, the combined field, fabric and isotopic evidence indicates that the orbicular cordierites are mafic cumulate rocks that crystallized from an isotopically homogeneous peraluminous magma. The contemporaneous leucogranitic melt was trapped between the orbicules and solidified as intercumulus material (Fig. 4). These features are common in basic plutonic complexes but extremely rare in granitic rocks.

Massive crystallization of cordierite on restitic cores followed by flow-driven accumulation of orbicules at shallow levels depleted the liquid in MgO, FeO, Al_2O_3 and MnO and increased the silica content to 74–76% (Figs 8 and 10). The decrease in the colour index of the normal facies of the monzogranite (FeO_t + MgO ~2%) to form leucogranite (FeO_t + MgO ~0·6%) is ascribed to cordieritite segregation from the granitic melt (Fig. 10). Crystallization of high-Mg cordierite reduced the ASI and depleted the MgO of the residual leucogranite melt (Fig. 9). It should be noted that the average CaO, Na_2O and K_2O of the leucogranite and the normal facies of the monzogranite are similar (Table 2b), indicating that feldspar fractionation was not significant. Quantitative evaluation of the cordierite fractionation must take into account the fact that orbicular cordierites are complex cumulates composed of magmatic cordierite and metapelitic restitic cores. Leucogranites may thus be formed by a single process that simultaneously involved (1) separation of an early formed hydrous mafic mineral by fractional crystallization and (2) separation of a restitic assemblage from the magma by a type of restite unmixing process (White & Chappell, 1977).

A least-squares fractionation model using the orbicular cordieritite as a cumulate assemblage provides a useful quantitative framework for this process (Table 2b). The modelled fractionation of this 'natural' composite cumulate involved the combined extraction of pure cordierite [parental magma = x leucogranite (1) + $(1 - x)$ cordierite] and restite [parental magma = x leucogranite (2) + $(1 - x)$ orbicular core] from a parental magma similar in composition to the average monzogranite (Table 2b). The main differences between the cumulate cordierite and restite end-members are in K_2O, TiO_2, P_2O_5 and CaO, as biotite, zircon and opaque minerals concentrate in the orbicular core and apatite in the cordieritites, respectively (Table 2). The proportion of shell/core is variable in the orbicules (Fig. 4), and therefore a typical orbicular cordieritite has been selected for modelling purposes (sample PIL-303). Despite these uncertainties, the least-squares calculations show that the parent monzogranitic magma can be well reproduced after ~8% extraction of the composite cumulate. Cordieritites therefore represent only ~8% of the monzogranitic magma.

Trace elements such as REE, Zr, Hf, Th and U that are concentrated in apatite and zircon—the main

accessory minerals of the cordieritite and biotitic restite, respectively—are also strongly depleted in the fractionated leucogranites (Fig. 10, Table 2). Zircon crystals largely occur armoured in the restitic biotite, so that Zr, U, Th and Hf are depleted in the fractionated leucogranites as a result of the coupled restite unmixing process that accompanied cordieritite formation. The high P_2O_5 content of the cordieritites is most probably related to the high solubility of apatite in peraluminous melts (Pichavant *et al.*, 1992), from which cordierite crystallized. The depleted REE patterns of the leucogranites, with positive Eu anomalies, can be explained by the combined extraction of the P_2O_5-rich cordieritite facies and restite as shown in Fig. 11a. Both the cordieritite and the biotite restite have higher light REE (LREE) and heavy REE (HREE) than the monzogranite. None the less, as the Eu content is similar in both melt and composite cumulate, the positive Eu anomaly in the leucogranitic liquid is developed by depletion of the remaining REE, which are partitioned in the composite cumulate. The REE pattern in the cordieritites is in turn directly related to the whole-rock P_2O_5 content (Fig. 11b). Coarse-grained cordieritites with low P_2O_5 contents show flat and depleted patterns without Eu anomalies, similar to those observed in purely magmatic cordierite (Bea, 1996). The total REE contents and the negative Eu anomalies of the cordieritites increase with the P_2O_5 content, from 0·02% P_2O_5 (0·05% normative apatite) in the coarse-grained cordieritites to a maximum of 1·1% P_2O_5 (2·5% normative apatite) in the fine-grained massive facies (Fig. 11b). The observed change of REE patterns in cordieritites corresponds to that from pure cordierite to an end component of pure apatite, which occurs in peraluminous granites (Fig. 11b). The large amount of modal apatite in the cordieritites is the main factor controlling the REE distribution during cordieritite extraction from peraluminous melts. Lensoid pegmatitic patches in the main monzogranite facies also developed depleted REE patterns with positive Eu anomalies (Fig. 11a) and plot on the Rb–Sr isochron (Rapela *et al.*, 1998*b*). This suggests that some fractionation occurred in the latest stages of crystallization of the monzogranitic magma, during which highly evolved melts segregate from crystal mush by a mechanism such as gas-driven filter pressing (Sisson & Bacon, 1999).

CONCLUSIONS

The El Pilón granite complex illustrates the rapid emplacement of highly peraluminous magmas in the upper crust at the start of the decompression stage of the Pampean orogeny. Field and petrological evidence indicates that the ascent of monzogranitic magmas was produced by feeder conduits that connected a source region located at $\sim$6 kbar, with the final emplacement level at 3·7 kbar. Fast injection of large amounts of highly peraluminous magmas at high level in the crust was critical for developing the late M_2 high dT/dP gradient that formed the cordierite diatexites and stromatites of the El Pilón complex. The conclusion that melts were able to migrate rapidly over long distances and accumulate at higher levels in the crust explains why granitic plutons have not been found in the neighbourhood of other melt-depleted migmatitic and granulitic terranes in the Sierras de Córdoba (Otamendi & Patiño Douce, 2001). This mechanism sharply contrasted with the slow diapiric ascent proposed for granites and migmatites in other high-T, low-P complexes (e.g. Barbey *et al.*, 1999).

Cordieritites appear at the top of conduits feeding into the floor of a laccolith-like body of a cordierite monzogranite. This hot, H_2O-undersaturated, highly peraluminous magma reached fluid-saturation conditions at the emplacement level, probably as a result of a rapid decompression and extensive assimilation of metapelitic country rock enclaves. This produced a marked fall in the liquidus temperature of the melt, which in turn destroyed crystallization nuclei, forcing crystallization to occur only on solid objects (Vernon, 1985), and provoked strong convection in the small magma chamber. High-Mg cordierite crystallized first in the magma, either on Bt + Sil schist restites (forming orbicular cordieritites) or at the side of the conduits as massive cordieritite. During the isobaric cooling, flow segregation of cumulate cordierite and restite decreased the colour index of the residual magma, developing leucogranites and highly evolved pegmatoids that are all in isotopic equilibrium (Nd and Sr). Again, this situation seems to be the antithesis of other water-undersaturated crust-derived granites emplaced by dykes, such as the Himalayan granites, in which heterogeneous initial isotopic ratios indicate that no significant magma mixing occurred during emplacement (Scaillet *et al.*, 1990).

ACKNOWLEDGEMENTS

Many thanks are due to J. L. Fernández Turiel for his help with the REE determinations (inductively coupled plasma mass spectrometry at the Instituto Jaume Almera, Barcelona) and Carlos Villaseca for providing unpublished data for Hercynian leucogranites. The authors also thank the journal reviewers M. Pichavant, J. Otamendi and F. Spear, and editor M. Wilson, for constructive comments that greatly improved the quality of the manuscript. This work was supported by grants PICT-4189 (FONCYT, Argentina), PIP-4148 (CONICET, Argentina) and CI1-CT92-0088 from the Commission of the European Communities. It is a contribution to IGCP Project No. 436 (Pacific Margin of Gondwana).

REFERENCES

Baldo, E. G. A., Demange, M. & Martino, R. D. (1998). Structural evolution of the Sierras de Córdoba (Argentina). *Tectonophysics* **267**, 121–142.

Barbey, P., Marignac, C., Montel, J. M., Macaudière, J., Gasquet, D. & Jabbori, J. (1999). Cordierite growth textures and the conditions of genesis and emplacement of crustal granitic magmas: the Velay Granite Complex (Massif Central, France). *Journal of Petrology* **40**, 1425–1441.

Bea, F. (1996). Residence of REE, Y, Th and U in granites and crustal protoliths; implications for the chemistry of crustal melts. *Journal of Petrology* **37**, 521–552.

Berman, R. G. (1991). Thermobarometry using multi-equilibrium calculations: a new technique, with petrological applications. *Canadian Mineralogist* **29**, 833–855.

Bouloton, J. (1992). Mise en évidence de cordiérite héritée des terrains transversés dans le pluton granitique des Oulad Ouaslam (Jebilet, Maroc). *Canadian Journal of Earth Sciences* **29**, 658–668.

Brown, M. (1998). Unpairing metamorphic belts: *P–T* paths and a tectonic model for the Ryoke Belt, southwest Japan. *Journal of Metamorphic Geology* **16**, 3–22.

Clarke, D. B. (1995). Cordierite in felsic igneous rocks: a synthesis. *Mineralogical Magazine* **59**, 311–325.

Clemens, J. D. (1998). Observations on the origin and ascent mechanisms of granitic magmas. *Journal of the Geological Society, London* **155**, 843–851.

Crawford, M. B. & Windley, B. F. (1990). Leucogranites of the Himalaya–Karakoram: implications for magmatic evolution within collisional belts and the study of collision-related leucogranite petrogenesis. *Journal of Volcanology and Geothermal Research* **44**, 1–19.

DePaolo, D. J., Linn, A. M. & Schubert, G. (1991). The continental crustal age distribution; methods of determining mantle separation ages from Sm–Nd isotopic data and application to the Southwestern United States. *Journal of Geophysical Research* **B96**, 2071–2088.

Dietrich, V. & Gansser, A. (1981). The leucogranites of the Bhutan Himalaya (crustal anatexis versus mantle melting). *Schweizerische Mineralogische und Petrographische Mitteilungen* **61**, 177–202.

Elliston, J. N. (1984). Orbicules: an indication of the crystallisation of hydrosilicates, I. *Earth-Science Reviews* **20**, 265–344.

Escuder Viruete, J., Hernaíz Huerta, P. P., Valverde-Vaquero, P., Rodríguez Fernández, R. & Dunning, G. (1998). Variscan syn-collisional extension in the Iberian Massif: structural, metamorphic and geochronological evidence from the Somosierra sector of the Sierra de Guadarrama (Central Iberian Zone, Spain). *Tectonophysics* **290**, 87–109.

Fantini, R., Gromet, L. P., Simpson, C. & Northrup, C. J. (1998). Timing of high-temperature metamorphism in the Sierras Pampeanas of Córdoba, Argentina: implications for Laurentia–Gondwana interactions. *Actas X Congreso Latinoamericano de Geología, Buenos Aires, Vol. 2*, 388–392.

Fuhrman, M. L. & Lindsley, D. H. (1988). Ternary-feldspar modeling and thermometry. *American Mineralogist* **73**, 201–216.

Gardien, V., Lardeaux, J. M., Ledru, P., Allemand, P. & Guillot, S. (1997). Metamorphism during late orogenic extension: insights from the French Variscan belt. *Bulletin de la Societé Géologique de France* **168**, 271–286.

Gordillo, C. E. (1974). Las rocas cordieríticas de Orcoyana y Cerro Negro–Soto (Córdoba). *Boletín de la Asociación Geológica de Córdoba* **2**, 90–100.

Gordillo, C. E. (1979). Observaciones sobre la petrología de las rocas cordieríticas de la Sierra de Córdoba. *Boletín de la Academia Nacional de Ciencias, Córdoba, Argentina* **53**, 3–44.

Gordillo, C. E. (1984). Migmatitas cordieríticas de la Sierra de Córdoba, condiciones fisicas de la migmatización. *Miscelánea de la Academia Nacional de Ciencias, Córdoba, Argentina* **68**, 1–40.

Gribble, C. D. (1968). The cordierite-bearing rocks of Haddo House and Arnage districts, Aberdeenshire. *Contributions to Mineralogy and Petrology* **17**, 125–136.

Gribble, C. D. & O'Hara, M. J. (1967). Interaction of basic magma and pelitic materials. *Nature* **214**, 1198–1201.

Hogan, J. P., Price, J. P. & Gilbert, M. C. (1998). Magma traps and driving pressure: consequences for pluton shape and emplacement in an extensional regime. *Journal of Structural Geology* **20**, 1155–1168.

Holtz, F., Johannes, W. & Pichavant, M. (1992). Peraluminous granites: the effect of alumina on the melt composition and coexistent minerals. *Transactions of the Royal Society of Edinburgh, Earth Sciences* **83**, 409–416.

Johannes, W. & Holtz, F. (1996). *Petrogenesis and Experimental Petrology of Granitic Rocks*. Berlin: Springer, 335 pp.

Kawano, Y. (1933). Chemical studies of the orbicular rocks from Minedera-yama. *Imperial Academy of Sciences, Japan, Proceedings* **9**, 613–616.

Kretz, R. (1983). Symbols for rock-forming minerals. *American Mineralogist* **68**, 277–279.

La Roche, H. (1992). Un homologue cationique du triangle Q–A–P (quartz–feldspath alcalin–plagioclase), figure majeure de la pétrologie des roches plutoniques. *Comptes Rendus de l'Académie des Sciences, Série II* **315**, 1687–1693.

Le Fort, P., Cuney, M., Deniel, C., France-Lanord, C., Sheppard, S. M. F., Upreti, B. N. & Vidal, P. (1987). Crustal generation of the Himalayan leucogranites. *Tectonophysics* **134**, 39–57.

Leveson, D. J. (1966). Orbicular rocks: a review. *Geological Society of America Bulletin* **77**, 409–426.

Martino, R., Kraemer, P., Escayola, M., Giambastiani, M. & Arnosio, M. (1995). Transecta de las Sierras de Córdoba a los 33°S. *Revista de la Asociación Geológica Argentina* **50**, 60–77.

Mathias, M. (1952). An unusual cordierite-rock from Upington, Cape Province. *Mineralogical Magazine* **29**, 936–945.

McMullin, D. W. A., Berman, R. G. & Greenwood, H. J. (1991). Calibration of the SGAM thermobaromenter for pelitic rocks using data from phase-equilibria experiments and natural assemblages. *Canadian Mineralogist* **29**, 889–908.

Miller, C. F. (1985). Are strongly peraluminous granites derived from pelitic sedimentary sources? *Journal of Geology* **93**, 673–689.

Montel, J. M., Marignac, C., Barbey, P. & Pichavant, M. (1992). Thermobarometry and granite genesis: the Hercynian low-*P*, high-*T* Velay anatectic dome (French Massif Central). *Journal of Metamorphic Geology* **10**, 1–15.

Moore, J. G. & Lockwood, J. P. (1973). Origin of comb layering and orbicular structure, Sierra Nevada Batholith, California. *Geological Society of America Bulletin* **84**, 1–20.

Otamendi, J. E. & Patiño Douce, A. E. (2001). Partial melting of aluminous metagreywackes in the northern Sierra de Comechingones, Central Argentina. *Journal of Petrology* **42**, 1551–1772.

Otamendi, J. E., Patiño Douce, A. E. & Demichelis, A. H. (1999). Amphibolite to granulite transition in aluminous greywackes from the Sierra de Comechingones, Córdoba, Argentina. *Journal of Metamorphic Geology* **17**, 415–434.

Pankhurst, R. J. (1969). Strontium isotope studies applied to petrogenesis in the basic igneous province of North-East Scotland. *Journal of Petrology* **10**, 116–145.

Pankhurst, R. J. & Rapela, C. W. (1998). Introduction. In: Pankhurst, R. J. & Rapela, C. W. (eds) *The Proto-Andean Margin of Gondwana. Geological Society, London, Special Publications* **142**, 1–9.

Pankhurst, R. J., Rapela, C. W. & Fanning, C. M. (2000). Age and origin of coeval TTG, I- and S-type granites in the Famatinian belt

of NW Argentina. *Transactions of the Royal Society of Edinburgh, Earth Sciences* **91**, 151–168.

Patiño Douce, A. E. (1996). Effect of pressure and H_2O content on the compositions of primary crustal melts. *Transactions of the Royal Society of Edinburgh, Earth Sciences* **87**, 11–21.

Patiño Douce, A. E. & Harris, N. (1998). Experimental constraints on Himalayan anatexis. *Journal of Petrology* **39**, 689–710.

Petford, N., Cruden, A. R., McCaffrey, K. J. W. & Vigneresse, J. L. (2000). Granite magma formation, transport and emplacement in the Earth's crust. *Nature* **408**, 669–673.

Phillips, G. N., Wall, V. J. & Clemens, J. D. (1981). Petrology of the Strathbogie batholith: a cordierite-bearing granite. *Canadian Mineralogist* **19**, 47–63.

Pichavant, M., Montel, J. M. & Richard, L. R. (1992). Apatite solubility in peraluminous liquids: experimental data and extension of the model of Harrison and Watson (1984). *Geochimica et Cosmochimica Acta* **56**, 3855–3861.

Puziewicz, J. & Johannes, W. (1988). Phase equilibria and compositions of Fe–Mg–Al minerals and melts in water-saturated peraluminous granitic magmas. *Contributions to Mineralogy and Petrology* **100**, 156–168.

Rapela, C. W., Pankhurst, R. J., Casquet, C., Baldo, E., Saavedra, J. & Galindo, C. (1998*a*). Early evolution of the Proto-Andean margin of South America. *Geology* **26**, 707–710.

Rapela, C. W., Pankhurst, R. J., Casquet, C., Baldo, E., Saavedra, J., Galindo, C. & Fanning, C. M. (1998*b*). The Pampean Orogeny of the southern proto-Andes: evidence for Cambrian continental collision in the Sierras de Córdoba. In: Pankhurst, R. J. & Rapela, C. W. (eds) *The Proto-Andean Margin of Gondwana. Geological Society, London, Special Publications* **142**, 181–217.

Read, H. H. (1923). The petrology of the Arnage district in Aberdeenshire; a study of assimilation. *Quarterly Journal of the Geological Society, London* **79**, 446–484.

Read, H. H. (1935). The gabbros and associated xenolithic complexes of the Haddo House district, Aberdeenshire. *Quarterly Journal of the Geological Society, London* **91**, 591–635.

Scaillet, B., France-Lanord, C. & Le Fort, P. (1990). Badrinath–Gangotri plutons (Garhwal, India): petrological and geochemical evidence for fractionation processes in a high Himalayan leucogranite. *Journal of Volcanology and Geothermal Research* **44**, 163–188.

Scaillet, B., Pêcher, A., Rochette, R. & Champenois, M. (1995*a*). The Gangotri granite (Garhwal Himalaya): laccolith emplacement in an extending collisional belt. *Journal of Geophysical Research* **100B**, 585–607.

Scaillet, B., Pichavant, M. & Roux, J. (1995*b*). Experimental crystallization of leucogranite magma. *Journal of Petrology* **36**, 663–705.

Schreyer, W., Gordillo, C. E. & Werding, G. (1979). A new sodian–beryllian cordierite from Soto, Argentina, and the relationship between distortion index, Be content and state of hydration. *Contributions to Mineralogy and Petrology* **70**, 421–428.

Sederholm, J. J. (1928). *On Orbicular Granites: Spotted and Nodular Granites etc., and on the Rapakivi Texture. Bulletin de la Commission Géologique de Finlande* **83,** 105 pp.

Sims, J. P., Ireland, T. R., Camacho, A., Lyons, P., Pieters, P. E., Skirrow, R. G., Stuart-Smith, P. G. & Miró, R. (1998). U–Pb, Th–Pb and Ar–Ar geochronology from the southern Sierras Pampeanas, Argentina: implications for the Palaeozoic tectonic evolution of the western Gondwana margin. In: Pankhurst, R. J. & Rapela, C. W. (eds) *The Proto-Andean Margin of Gondwana. Geological Society, London, Special Publications* **142**, 259–281.

Sisson, T. W. & Bacon, C. R. (1999). Gas-driven filter pressing in magmas. *Geology* **27**, 613–616.

Spear, F. S., Kohn, M. J. & Cheney, J. T. (1999). *P–T* paths from anatectic pelites. *Contributions to Mineralogy and Petrology* **134**, 17–32.

Ugidos, J. M. (1988). New aspects and considerations on the assimilation of cordierite-bearing rocks. *Revista de la Sociedad Geológica de España* **1**, 129–133.

Ugidos, J. M. & Recio, C. (1993). Origin of cordierite-bearing granites by assimilation in the Central Iberian Massif (CIM), Spain. *Chemical Geology* **103**, 27–43.

Vernon, R. H. (1985). Possible role of superheated magma in the formation of orbicular granitoids. *Geology* **13**, 843–845.

Villaseca, C., Barbero, L. & Herreros, V. (1998*a*). A re-examination of the typology of peraluminous granite types in intracontinental orogenic belts. *Transactions of the Royal Society of Edinburgh, Earth Sciences* **89**, 113–119.

Villaseca, C., Barbero, L. & Rogers, G. (1998*b*). Crustal origin of Hercynian peraluminous granitic batholiths of Central Spain: petrological, geochemical and isotopic (Sr, Nd) constraints. *Lithos* **43**, 55–79.

White, A. J. R. & Chappell, B. W. (1977). Ultrametamorphism and granitoid genesis. *Tectonophysics* **43**, 7–22.

Williamson, B. J., Shaw, A., Downes, H. & Thirlwall, M. F. (1996). Geochemical constraints on the genesis of Hercynian two-mica leucogranites from the Massif Central, France. *Chemical Geology* **127**, 25–42.

Yoshiki, B. (1933). Petrographic notes on the orbicular rocks from Minedera-Yama. *Imperial Academy of Sciences, Japan, Proceedings* **9**, 609–612.